Polymer Testing 143 (2025) 108709

Contents lists available at ScienceDirect

Polymer Testing

journal homepage: www.elsevier.com/locate/polytest

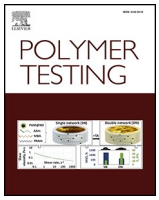

3D/4D printed bio-composites reinforced by bamboo charcoal and continuous flax fibres for superior mechanical strength, flame retardancy and recoverability

Mahdi Bodaghi [a,*], Kaveh Rahmani [a], Mohammadreza Lalegani Dezaki [a], Callum Branfoot [b], Jon Baxendale [b]

[a] Department of Engineering, School of Science and Technology, Nottingham Trent University, Nottingham, NG11 8NS, UK
[b] Engineering Operations, National Composites Centre, Bristol, BS16 7FS, UK

ARTICLE INFO

Keywords:
Continuous flax fibre
Bamboo charcoal
Shape memory polymer
Meta-bio-composite
Flame retardancy
3D/4D printing

ABSTRACT

This study explores development and 3D/4D printing of environmentally friendly bio-composites with enhanced mechanical properties, flame retardancy, and shape memory capabilities. Composite filaments were created by incorporating polylactic acid (PLA) with bamboo charcoal (BC) and then printed using a modified printer equipped with a dual-feed system to accommodate both PLA/BC filaments and continuous flax fibres (CFF). SEM revealed strong fibre-matrix bonding with minimal voids, indicating good interfacial adhesion. Bio-composite properties were characterised through DMA, tensile, three-point bending, flammability, and shape-memory effect tests. Adding 3 wt% BC and CFF significantly increased the tensile strength by 248 % and the flexural strength by 207 % compared to pure PLA. Flame retardancy properties were notably improved, with a 50 % reduction in the burning rate, and underwriters' laboratories (UL-94) rate and limiting oxygen index (LOI) reached to V-1 rating and 36.8%vol, respectively. DMA tests showed an increase in storage modulus, indicating improved stiffness. Shape memory tests under cold/hot programming protocols demonstrated efficient shape fixation with shape recovery ratios reaching up to 98.9 % for pure PLA and 89 % for PLA/BC/CFF for hot programming. Finally, a conceptual meta-bio-composite was 4D printed, showcasing key achievements such as quasi-zero stiffness, constant force behaviour, enhanced energy absorption/dissipation, and excellent recoverability and reusability. This highlights their potential for applications requiring durability, safety, comfort, and sustainability in sectors such as automotive, aerospace, logistics, construction, and furniture.

1. Introduction

3D printing technology, particularly fused filament fabrication (FFF), is emerging as a key technology for producing advanced composite materials. While 3D-printed polymers and short fibre-reinforced composites often have modest mechanical properties due to porosity and low fibre content, continuous fibre-reinforced composites offer superior mechanical performance, making them suitable for structural applications. Van der Klift et al. [1] integrated continuous fibres through the FFF process and 3D printed materials with competitive mechanical properties, opening new opportunities for creating high-performance thermoplastic composites. Tóth et al. [2] studied flexural stiffness in 3D-printed continuous fibre-reinforced composites, focusing on different matrix fill ratios and layer arrangements. They evaluated how flexural properties were influenced by these parameters and found that the highest strength and stiffness were achieved with the top/bottom layer arrangement. Heidari-Rarani et al. [3] demonstrated significant improvements in the tensile and bending strengths of continuous carbon fibre-reinforced polylactic acid (PLA) compared to pure PLA, with increases of up to 35 % and 108 %, respectively.

Continuous fibre-reinforced composites typically use glass, carbon, or Kevlar fibres, but environmental concerns have increased interest in bio-based composites with natural fibres [1,4]. To enhance sustainability and reduce reliance on synthetic fibres in modern composites, significant attention has recently been directed toward the use of natural fibres. They are recognized as attractive alternatives to synthetic fibres due to their biodegradable properties and low environmental impact during production and use [5,6]. 3D printing, on the other hand,

* Corresponding author.
E-mail address: mahdi.bodaghi@ntu.ac.uk (M. Bodaghi).

https://doi.org/10.1016/j.polymertesting.2025.108709
Received 29 November 2024; Received in revised form 6 January 2025; Accepted 16 January 2025
Available online 20 January 2025

presents a valuable opportunity to develop these bio-composites alongside synthetic counterparts. Replacing synthetic fibres with natural fibres in filament 3D printing can reduce greenhouse gas emissions associated with synthetic fibre production and help address current pollution problems [7]. These materials have demonstrated high strength and, due to their non-carcinogenic nature and safety during manufacturing and handling, offer environmental and health benefits. Recent research has focused on studying the mechanical properties of natural fibre-reinforced composite materials because of their promising mechanical behaviour [8,9].

Among the natural fibres that have garnered considerable interest in the composite industry are flax, hemp, and bamboo [10,11]. These fibres not only improve the mechanical properties of base materials but also help reduce environmental impacts. One of the prominent natural resources with high potential for producing composite materials is bamboo. Due to its rapid growth rate, desirable mechanical strength, and environmental compatibility, bamboo is recognized as one of the best options for producing sustainable materials [12,13]. Numerous studies have shown that using bamboo in the form of powder, short fibres, or bamboo charcoal (BC) enhances the mechanical, thermal, and even optical properties of base materials like PLA [14,15]. For example, Ho et al. [16] used bamboo charcoal particles to reinforce PLA and observed that at various weight percentages from 2.5 % to 10 %, the tensile strength, flexural strength, and ductility of PLA composites increased significantly. These results demonstrate the high potential of bamboo as a natural reinforcing material in the development of sustainable composites. Additionally, continuous flax fibre (CFF) has gained attention as a sustainable resource for producing various materials, especially composites. Flax is an excellent material for sustainable product manufacturing because of its rapid growth, minimal need for water and chemicals, and biodegradability [17]. Using CFF instead of synthetic fibres not only reduces greenhouse gas emissions but also improves the product's lifecycle and lowers energy consumption during production [12]. Flax, as a renewable resource, plays a crucial role in preserving natural resources and reducing the environmental impacts of manufacturing industries [12]. Letcher et al. [18] studied the tensile properties of CFF/PLA composites with a fibre volume content of 30.4 %. They found that the longitudinal properties of the CFF/PLA composites improved substantially compared to pure PLA, with a 7-fold enhancement in stiffness and a 4.5-fold increase in strength. Duigou et al. [19] proposed producing continuous flax fibre-PLA bio-composites by a co-extrusion process and optimised the mechanical properties to achieve improved tensile modulus and strength. Zhang et al. [8] developed continuous flax fibre reinforced plastic composite parts using a five-axis 3D printer based on FFF technology. They reported that the tensile strength and Young's modulus of CFFRP increased by 89 % and 73 %, respectively, compared to PLA filaments. Additionally, the flexural strength and modulus improved by 211 % and 224 %, respectively.

Plastic materials, due to their high flammability, have always posed safety challenges in various industries. In many industrial products especially structural components and applications involving heat, fire- and flame-retardants are of great importance. Therefore, the use of flame-retardant materials is essential to meet safety standards [20]. Additionally, industries involved in plastics are seeking environmentally friendly materials with high flame retardancy [21,22]. To address this issue, recent research efforts have focused on improving the flame-retardant and mechanical properties of PLA by combining it with various materials. These studies have proposed different strategies to enhance flame retardancy in PLA, leading to greater flame retardancy but often with reduced strength [23,24]. Zhang et al. [25] investigated the effect of adding 10 to 30 wt% of phosphate- and urea-modified bamboo charcoal (BC-m) to PLA and observed that this combination significantly improved flame retardant. However, the mechanical strength of the composites slightly decreased. In another study, Li et al. [26] developed a flame retardant system using modified BC along with a natural adhesive and chitosan for PLA. This system also increased flame retardancy but was accompanied by a slight decrease in the mechanical strength. Therefore, improving these properties in PLA-based bio--composites is of great importance. In this context, PLA-based bio--composites reinforced with natural fibres have attracted attention for flame retardancy, especially in automotive interior parts and packaging [27,28].

Despite advancements in flame-retardant and mechanically enhanced PLA composites, there remains a significant gap in the literature regarding the simultaneous improvement of mechanical strength, flame retardancy, printability, and shape memory capabilities using sustainable, natural additives. Existing research typically focuses on enhancing one of these aspects while sacrificing another. For instance, while adding flame-retardant materials improves flame retardancy, this often leads to diminished mechanical properties. Similarly, while continuous fibre reinforcements, such as flax fibres, have been shown to significantly improve mechanical strength, their effect on flame retardancy and printability, particularly in 3D printing processes, has not been fully investigated. Furthermore, shape memory polymer bio-composites (SMPBs), which possess the ability to recover their shape under thermal programming, have not yet been fully explored in the context of bio-composites reinforced with natural fibres and flame-retardant particles. SMPBs produced via 3D/4D printing offer an additional advantage by allowing deformed objects to recover their original shape through cold and hot programming (CP/HP) protocols. This capability reduces material consumption, extends the product's lifecycle, and supports the principles of sustainable manufacturing and the circular economy. Such materials are particularly valuable for industries such as automotive, aerospace, logistics, construction, and furniture, where reusability, durability, and safety are critical.

This study addresses these gaps by developing a novel flame-retardant system for PLA-based bio-composites that incorporates both continuous flax fibres and bamboo charcoal particles. By leveraging the combined properties of CFF and BC, this research enhances the mechanical strength, flame retardancy properties, and printability of the bio-composites, while also integrating the shape memory capabilities offered by 4D printing technology. The combination of these features makes these materials suitable for applications that demand both structural integrity and environmental sustainability. As demonstrated in this study, adding CFF and BC to PLA not only improves flame retardancy properties but also significantly enhances the mechanical properties of the composite, with increases in tensile and flexural strength. Moreover, the shape memory features of the composites allow for the recovery of deformed objects, enabling multiple uses and reducing the material waste. Fig. 1 illustrates the complete workflow of bio-composite development, including PLA and BC material preparation, filament extrusion, 3D printing with CFF reinforcement, and potential applications in meta-structures such as flame-retardant furniture and automotive seats. By combining natural flame-retardant particles and continuous natural fibres with the added functionality of shape memory, this study presents a new class of PLA-based bio-composites suitable for high-performance and sustainable applications. These findings contribute to advancing bio-composite technologies and open new possibilities for environmentally responsible manufacturing practices.

2. Materials

2.1. Polylactic acid

Semi-crystalline PLA Nature Works 4043D pellets produced by RESINEX Company, an eco-friendly thermoplastic polymer derived from renewable resources, were used as a matrix with shape memory effect (SME) properties as seen in Fig. 2a. This polymer can memorise shape and is widely used in 3D/4D printing. The melting point of this material ranges from 150 to 165 °C, and glass transition temperature (T_g) of this polymer is between 55 and 65 °C, and its melting temperature was

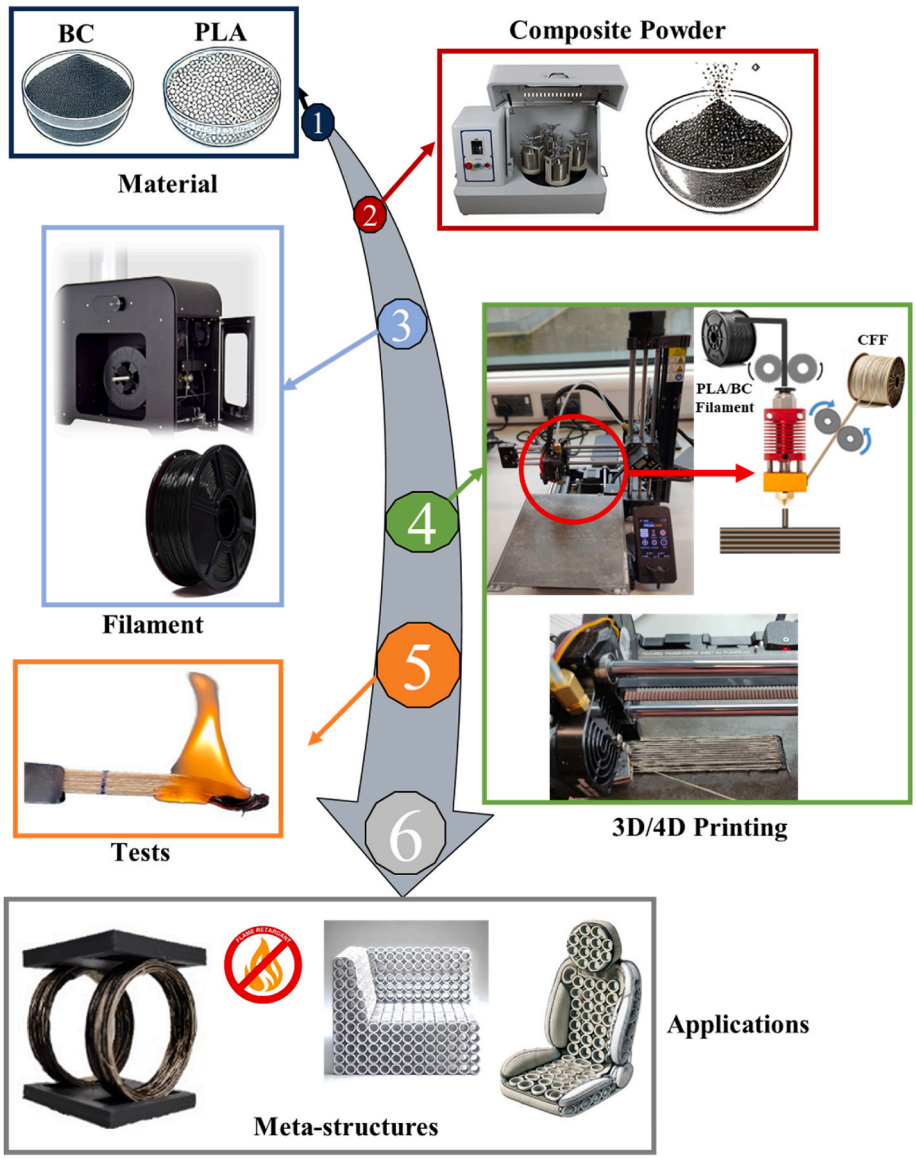

Fig. 1. A workflow of PLA/BC/CFF bio-composite from development to testing and then potential applications. It includes material preparation, composite powder mixing, filament extrusion, 3D/4D printing with CFF reinforcement, testing, and applications in meta-structures like flame retardant furniture and automotive seats.

reported to be 200 °C [29].

2.2. Bamboo charcoal powder

BC particles, a natural plant resource, were provided by Takesumi Ltd. (Japan) and were used as reinforcement to improve the matrix flame retardancy, Fig. 2b. The development of composites that use natural and biodegradable elements like BC is becoming more popular as the use of environmentally sustainable resources and techniques becomes more important [16,30]. Extracted from the bamboo plant, BC is relatively cheap, abundant, renewable, non-toxic, and stable. It is utilised in many different industries, including food processing, cosmetics, pharmaceuticals, and health-related items.

2.3. Continuous flax fibre

CFF, another natural plant resource, was supplied by Bobbin Lace Linen Threads and used as reinforcement to improve the structural strength. Flax (Linum usitatissimum) is one of the most widely used and oldest bio-fibres, historically employed for extraction, spinning, and textile production as illustrated in Fig. 2c. High-quality, industrially produced flax yarns are available in a variety of linear densities [7]. Due to their superior tensile properties, these fibres are considered among the best available natural materials. The selected flax yarn (fine unwaxed natural linen) has a linear density of 38 Tex × 2 2-ply thread.

3. Manufacturing and methods

Fig. 3 illustrates the key steps starting from raw materials PLA and BC particles, ball milling, composite filament extrusion, to 3D printing of BC/PLA bio-composite filaments reinforced by the CFF. Details of each step are described below.

3.1. Filament extrusion process

Despite being hydrophobic, PLA pellets and BC particles are moisture sensitive. In order to reduce excess moisture before the extrusion process, BC particles and PLA pellets were combined and dried in a hot-air drier at 70 °C for 24 h. After this step, various mixtures were prepared by adding BC particles to PLA at weight percentages of 0, 1.5, 3, and 5 wt%,

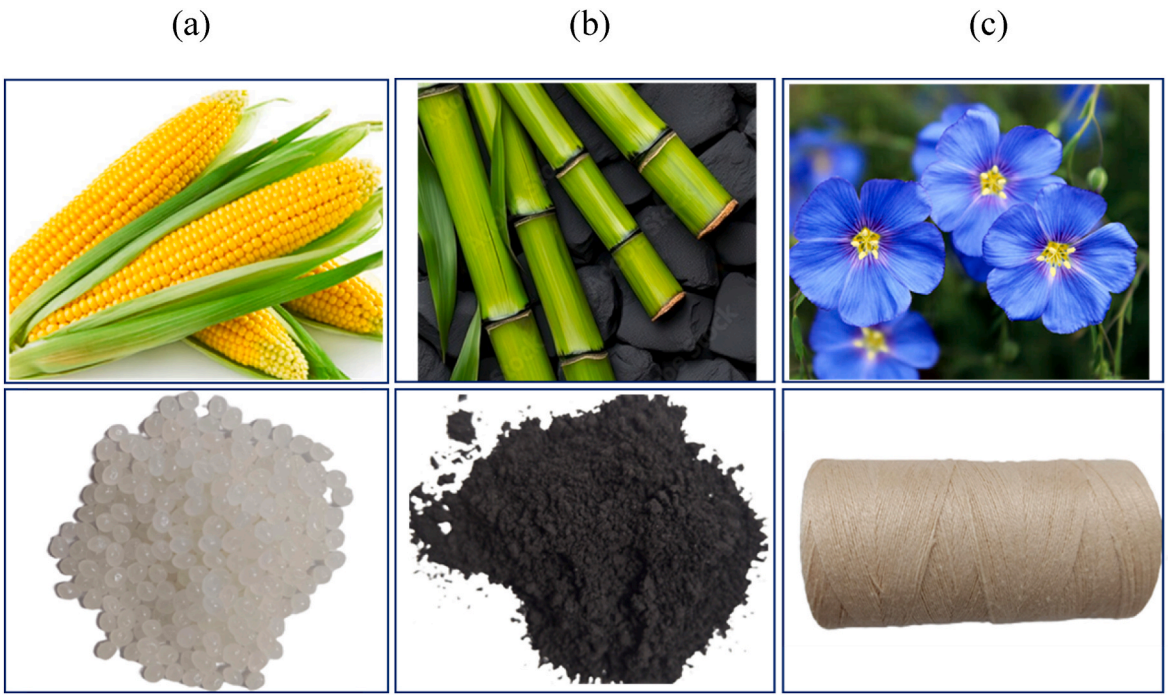

Fig. 2. Bio-composite feedstocks and their plant origins: (a) polylactic acid (PLA) pellets, (b) bamboo charcoal (BC) powder, (c) continuous flax fibre (CFF).

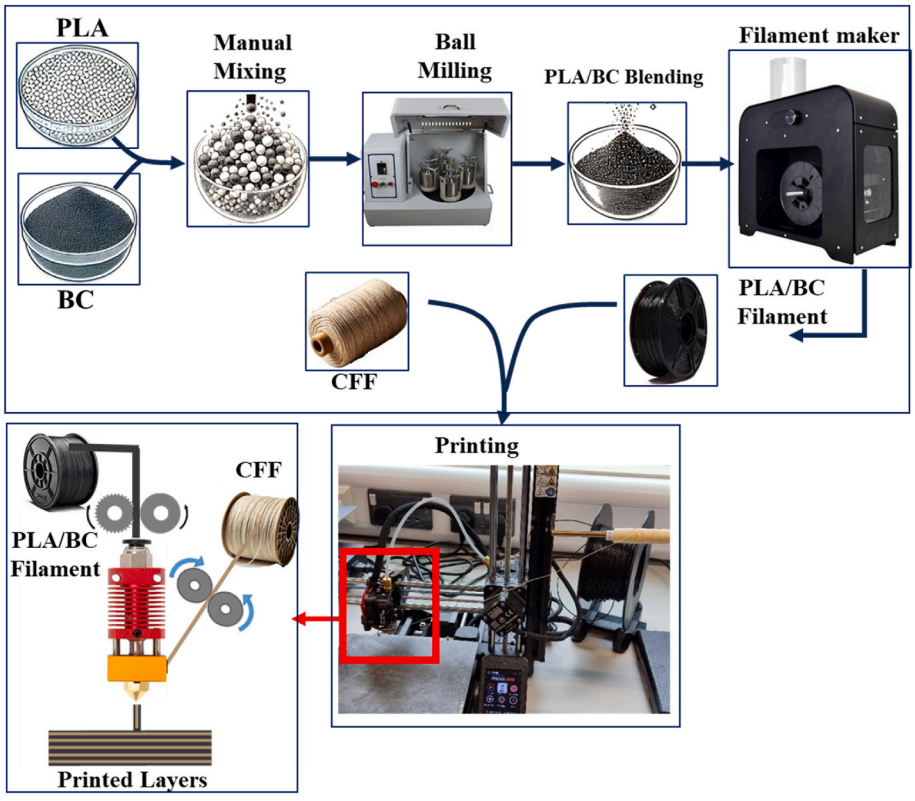

Fig. 3. Bio-composite development from composite materials preparation to 3D printing. Key steps start from raw PLA and bamboo charcoal particles to ball milling, composite filament extrusion, and finally implementing a modified FFF 3D printer to fabricate continuous natural fibre-reinforced polymers.

as shown in Fig. 4a. These were mixed in a planetary ball mill to reach a uniform distribution of BC particles in the PLA pellets as demonstrated in Fig. 4b. The PLA/BC mixtures were then extruded using a single extruder device (3devo, Netherlands) to fabricate filaments with a diameter of 1.75 mm, which was used for all printed samples. Processing parameters such as temperature and extrusion rate were adjusted to produce filaments with minimal defects and minimal variations in diameter. Table 1 shows the extrusion parameters that were used for the PLA/BC bio-composite filaments.

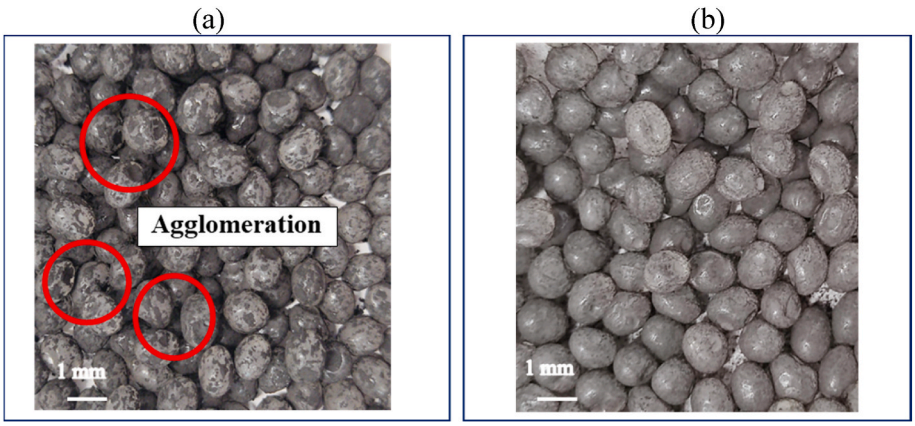

Fig. 4. Mixed PLA and bamboo charcoal: (a) before and (b) after planetary ball milling.

Table 1
PLA/BC filament extrusion process parameters.

Parameters	Value
Extrusion temperature at heat zone 1 (°C)	170
Extrusion temperature at heat zone 2 (°C)	190
Extrusion temperature at heat zone 3 (°C)	185
Extrusion temperature at heat zone 4 (°C)	170
Die temperature (°C)	185
Fan speed (m/s)	100
Extrusion rotation speed (rpm)	3.5
Filament diameter (mm)	1.75

3.2. Extruder development and printing process

To develop polymer composites reinforced with natural CFF, a specially designed extruder for FFF printers and a single nozzle 3D printer based on FFF technology were used. In this research, the Original Prusa MINI+ 3D printer was used to print samples. The main improvement in this printer was modifying a feeding channel for CFF to enter the extruder. It was designed to simultaneously feed both the PLA/BC composite filament and the CFF. It then combined the CFF and the molten composite plastic and deposited them simultaneously. Fig. 3 shows a detailed schematic of the modified extruder's operation, where the PLA/BC composite and CFF enter the extruder through two separate channels and are then combined and extruded through a single-output nozzle.

All samples were produced using fixed printing parameters as listed in Table 2. The extruder with a diameter of 2 mm was used to fabricate all test samples, and no issues like clogging occurred during the process. PLA filaments reinforced with varying percentages of BC are labelled as PLA/BC by wt%. The PLA samples reinforced with BC are denoted as PLA/BC. Also, PLA and PLA/BC samples reinforced with CFF are denoted as PLA/CFF and PLA/BC/CFF, respectively.

Table 2
Printing parameters set in this study.

Parameters	Value
Nozzle diameter (mm)	2
Layer thickness (mm)	0.2
Printing speed (mm/s)	30
Infill density (%)	100
Printing pattern	Linear
Nozzle temperature (°C)	215
Bed temperature (°C)	60

4. Characterisation

4.1. Mechanical properties

The mechanical properties of the samples were evaluated through tensile and three-point bending tests using a Shimadzu AG-X plus machine. The tensile test for pure PLA samples, PLA/BC samples without fibre reinforcement, and PLA/BC/CFF and PLA/CFF samples was performed as dictated by ASTM D638 and D3039, respectively. The tensile speed in these tests was 5 mm/min with a distance of 100 mm between the grips [31,32]. Additionally, the three-point bending test of the printed samples was conducted in accordance with ASTM D790 at a displacement rate of 5 mm/min and a span of 50 mm between the supports [33]. All tests were performed without conditioning under ambient laboratory conditions on five samples from each group, and average values were reported for each series of tests. To maximise their strength, all samples were printed along the longitudinal direction. Fig. 5a shows the 2D drawing of samples based on ASTM standards. Also, Fig. 5b and c displays the test specimens and the printed samples with magnified images, respectively.

4.2. Microstructural evaluation

To examine the microstructure, fracture surfaces, and fibre distribution in the samples, a scanning electron microscope (SEM) model JSM-7100 F LV FEG was used. Before imaging, the samples were coated with a thin layer of gold to obtain clearer images.

4.3. Dynamic mechanical analysis

The glassy-to-rubbery phase transition behaviour of 3D-printed SMPBs depends on two key thermodynamic variables: the storage modulus and glass transition temperature (i.e., T_g). It is essential to investigate the effect of adding natural fibres and BC particles on the storage modulus and T_g of semi-crystalline PLA plastic. In this study, 3D/4D printed pure PLA samples and composites reinforced with natural fibres and BC particles were subjected to dynamic thermo-mechanical examination using a dynamic mechanical analyser (DMA) machine (DMA 8000 PerkinElmer). The prepared samples had the following measurements: 30 mm length, 8 mm width, and 1 mm thickness. The temperature range under examination was 20–80 °C, with a heating rate of 5 °C/min and a frequency of 1 Hz.

4.4. Melt flow index (MFI)

In accordance with ASTM D1238-04, the PLA and PLA/BC composite's MFI was determined using melt flow index machine at 190 °C and 2.16 kg of load.

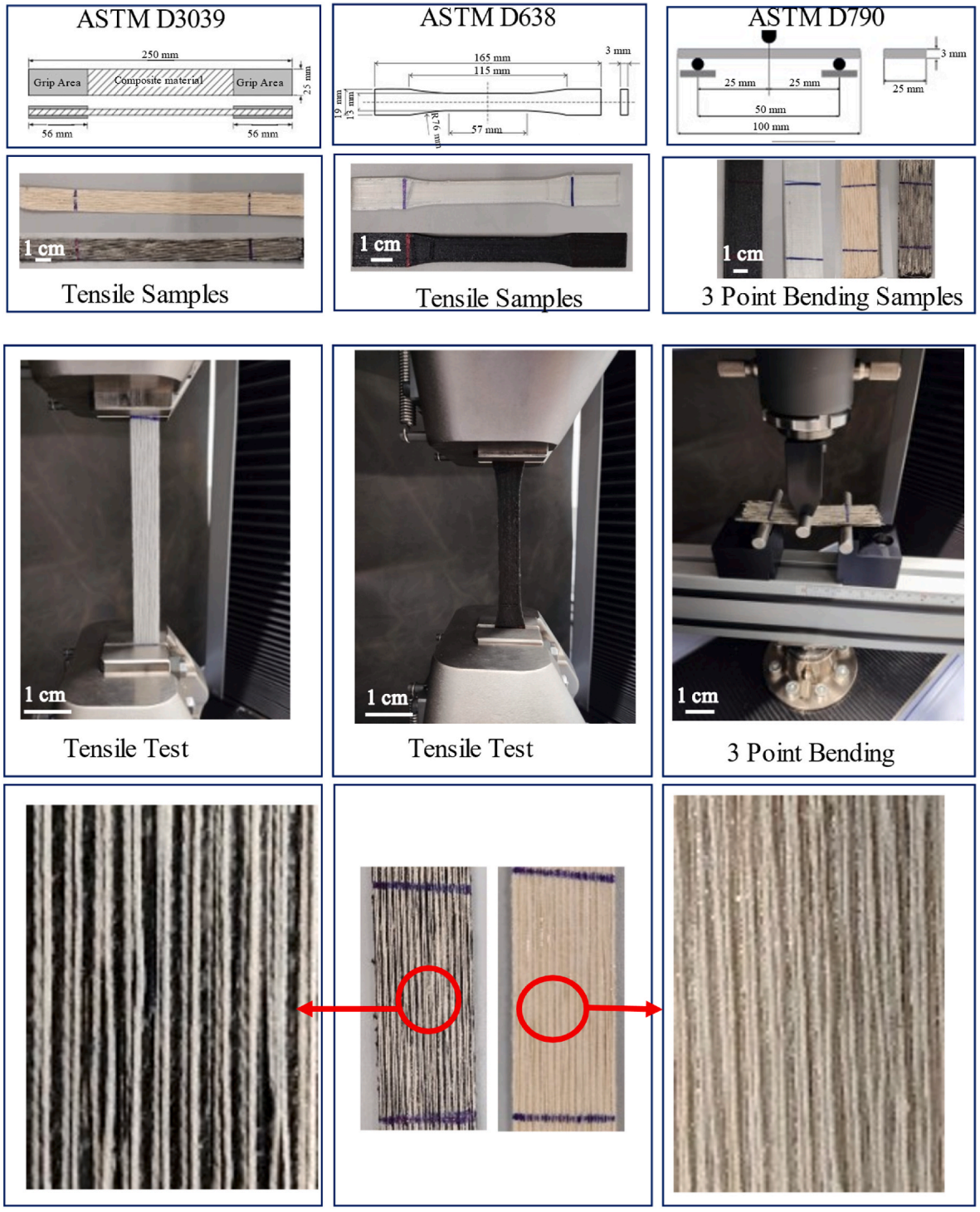

Fig. 5. (a) Drawing of samples based on ASTM standards, (b) images of testing samples printed following ASTM standards and (c) magnified images of fibres in samples.

4.5. Preparation of flame-retardant composites

The flammability properties of the composites were comprehensively characterised by a combination of underwriters' laboratories (UL-94) horizontal and vertical burning tests, limiting oxygen index (LOI) measurements, and cone calorimeter tests (CCTs). The methodologies employed are detailed below.

(a) Horizontal Burning Test:

The flammability of the samples was evaluated consistent with ASTM D635-22 to determine the burning rate and burning duration of plastics in a horizontal position [34,35]. Printed samples installed horizontally were placed in a fume hood and marked at distances of 25 mm and 100 mm from one end. A gas burner was then used to apply heat to the end of the sample so that the flame penetrated to a depth of 6 mm, and timing began simultaneously. The time and distance of flame propagation from the 25 mm mark to the 100 mm mark were recorded. The burning rate of the composites was determined using the following equation:

$$V = \frac{60 \times l}{t} \quad (1)$$

where L is burned length (mm), t is burning time (sec), and V is burning rate (mm/min). The burning rate for each sample was calculated in this way to evaluate their flammability performance [36,37].

(b) Vertical Burning Test:

To classify materials based on their ability to extinguish flames and resist dripping during combustion, vertical burning tests were conducted using a UL-94 vertical flame chamber instrument in accordance with ASTM D3801. The LOI values, indicative of the minimum oxygen concentration required to sustain combustion, were measured using an oxygen index meter following ASTM D2863 standard. This assessment provided critical insights into the inherent flame-retardant capabilities of the composite materials. To evaluate the combustion behaviour and heat release characteristics, CCTs were performed in accordance with

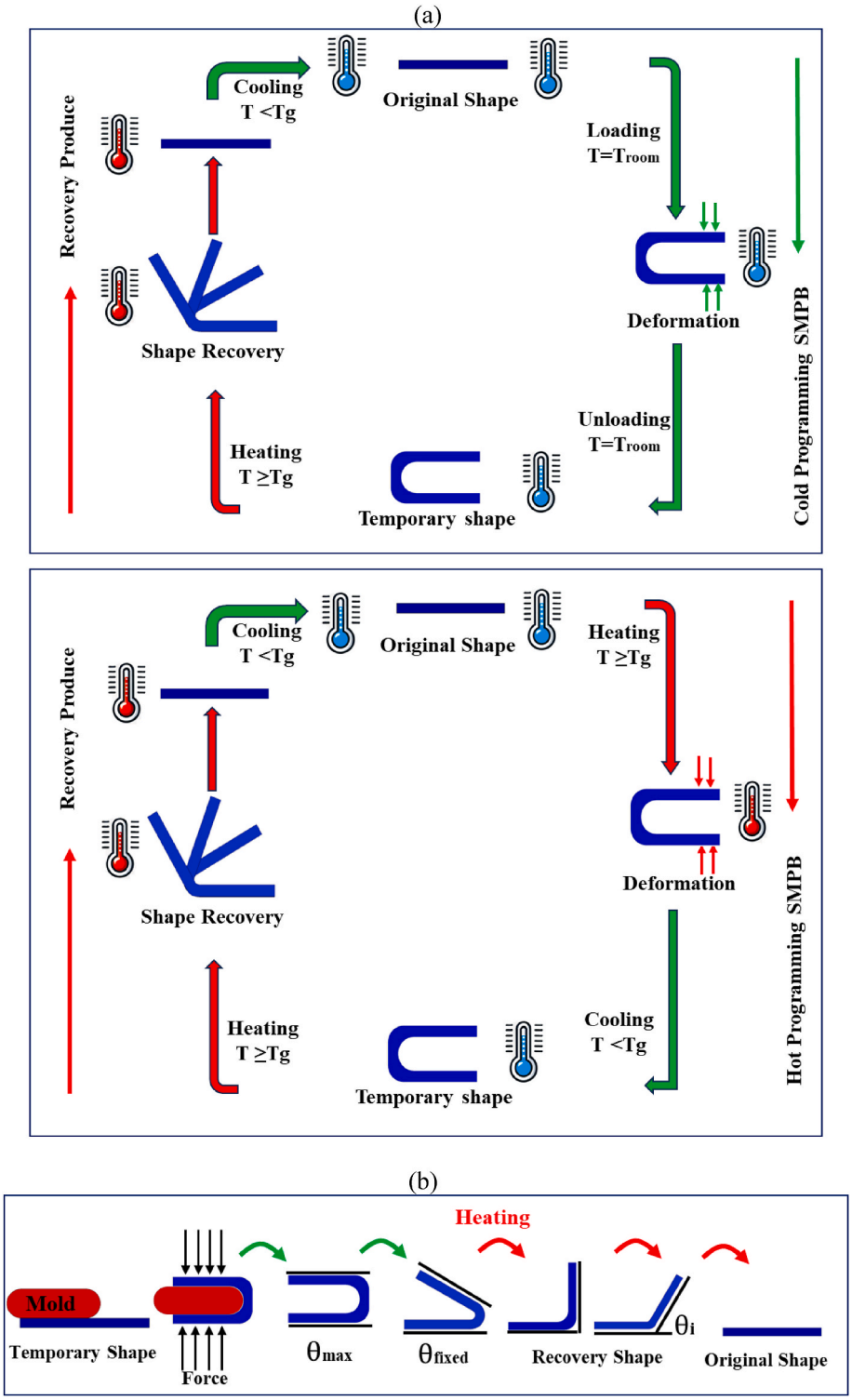

Fig. 6. (a) CP and HP procedures applied to the shape memory polymer bio-composites SMPBs, (b) bending angle recorded at various steps.

ISO 5660 standard. Specimens with a thickness of 3 mm were subjected to a heat flux of 35 kW/m^2. The CCTs provided detailed data on parameters such as heat release rate, total heat released, and time to ignition, which are essential for understanding the fire performance of the composites under realistic fire conditions.

4.6. Shape memory tests

The capability of the printed bio-composites to recover to the original shape under thermal stimulation is evaluated using CP/HP protocols, as shown schematically in Fig. 6a. This test aims to study the effect of BC and CFF on the SME features of the PLA matrix 3D-printed samples of 30 mm in length, 8 mm in width, and 1 mm in thickness. Experiments was performed in triplicate and average values were reported for each series of tests. In the HP approach, they were first heated to a specific temperature beyond T_g. The samples were further deformed by applying sufficient force into a mould with a diameter of 20 mm, as demonstrated in Fig. 6b. The maximum bending angle applied was recorded as θ_{max} in the shape fixation step, see Fig. 6b. After applying external force and deformation, the samples were cooled to the room temperature, and once stabilised, the mould and force were removed. The fixed angle was designated as θ_{fixed}. Then, the samples were reheated gradually to achieve the maximum recovery and then cooled down. The final bending angle θ_i was carefully recorded. In the CP method, the samples were first deformed at room temperature to achieve θ_{max}, and then the force was released to record the fixed angle θ_{fixed} due to residual inelastic strains that remained in the material. Following a similar heating-cooling trend applied in the HP method, θ_i was measured indicating a partial/full recovery of those inelastic deformations. The shape fixation and recovery ratios were calculated based on the recorded angles:

$$Shape\ fixity\ (sf) = \frac{\theta_{fixed}}{\theta_{max}} \times 100 \tag{2}$$

$$Shape\ recovery\ (sr) = \frac{\theta_{max} - \theta_i}{\theta_{max}} \times 100 \tag{3}$$

The heating of the samples was performed using a heat gun at the specified temperature. The samples were positioned vertically and fastened at one end. The FLIR E5-XT thermal camera, was used to record and document the shape recovery sequence.

5. Results and discussion

5.1. Mechanical properties

In this section, the mechanical properties of the printed bio-composites are examined. First, the tensile properties of 3D-printed PLA composites reinforced with BC particles at weight percentages of 0 %, 1.5 %, 3 %, and 5 % are evaluated according to ASTM D638 standard. As the BC weight percentage increased, the tensile strength of the PLA/BC composites also increased, as shown in Fig. 7. A similar conclusion was made by Fu et al. [38] who observed that the BC particles in PLA reduce the mobility of PLA structures, resulting in an increase in stiffness and Young's modulus of the BC/PLA composites. Fig. 7 also reveals that the highest tensile strength is observed in samples containing 3 % by weight of BC, which is 33 % higher than that of pure PLA. However, further increasing the BC content led to a decrease in tensile strength. Two possible explanations for this are: 1) Excessive addition of BC particles may lead to reduced filament uniformity and cause problems in the printing process, preventing the printer from producing high-density samples; 2) The aggregation of BC particles and the formation of BC clusters in the PLA matrix may result in partial separation of micro-voids between particles and the polymer and it can disrupt the stress transfer when the tensile force is applied.

Next, after figuring out the maximum tensile strength of the PLA/BC composites, the PLA/BC filament containing 3 % by weight of BC (PLA/3%wt BC) is selected as the composite matrix and reinforced with continuous flax fibres (CFF) to improve its mechanical properties. The mechanical properties, including tensile strength and three-point bending, of the bio-composites reinforced with CFF are evaluated and analysed. Fig. 8a demonstrates the tensile behaviour of the printed PLA bio-composites reinforced with BC particles and CFF, as well as the unreinforced samples. As can be seen in the figure, the natural flax fibres significantly enhance the strength of the printed samples. Fig. 8b presents the results of the ultimate tensile strength. It is found that, among these samples, PLA/BC/CFF with an average tensile strength of 120 MPa has the highest strength compared to PLA, PLA/CFF, and PLA/BC. The tensile strength of PLA/BC/CFF is approximately 161 % and 248 % higher than that of PLA/BC and pure PLA, respectively, and the tensile strength of PLA/CFF is about 84 % and 145 % higher than that of PLA/BC and pure PLA, respectively. In contrast, pure PLA depicts lower tensile strength compared to the other three samples. The observed increase in tensile strength of PLA/BC/CFF can be attributed to the effective load transfer at the fibre-matrix interface and the ductility of the continuous flax fibres, which delay cracking.

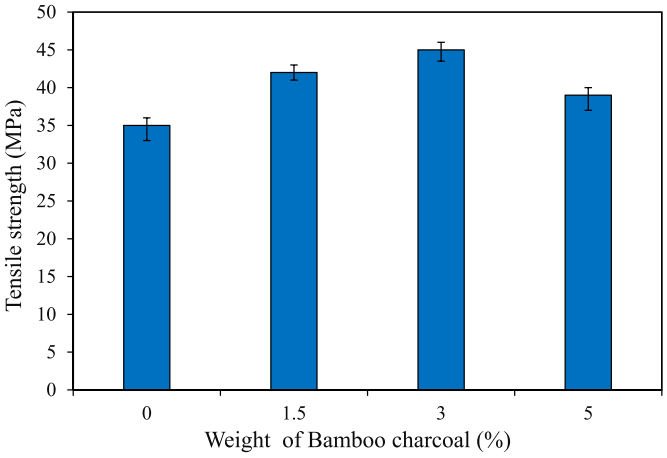

Fig. 7. Tensile strength of pure PLA and PLA/BC composites with various bamboo charcoal contents.

5.2. Three-point bending test

In this section, the three-point bending performance of the printed samples is evaluated. Fig. 9a presents the three-point bending strength results of all four different types of materials. As can be seen in Fig. 9a, adding CFF and BC particles to PLA increases the three-point bending strength. The results for PLA and PLA/BC samples, similar to equivalent tensile tests, show lower three-point bending strength compared to samples containing fibres due to the absence of long fibres. The three-point bending strength of PLA/BC/CFF is 207 %, 165 %, and 27 % higher than PLA, PLA/BC, and PLA/CFF, respectively. In three-point bending tests, like tensile tests, PLA/BC/CFF demonstrates superior mechanical properties compared to other printed samples. The three-point bending, and tensile strengths of the samples are compared in Fig. 9b. As can be observed, the tensile strength of the PLA/BC/CFF sample is 18 % higher than its three-point bending strength. The pure PLA sample without reinforcement of BC particles and CFF exhibits the lowest tensile and three-point bending strengths.

5.3. Microstructure study

In this section, the microstructure and flax fibre volume fraction in the developed bio-composites are examined using scanning electron microscopy (SEM). Fig. 10a exhibits SEM images of the microstructure of the flat surfaces and fracture surfaces of PLA/BC/CFF tensile

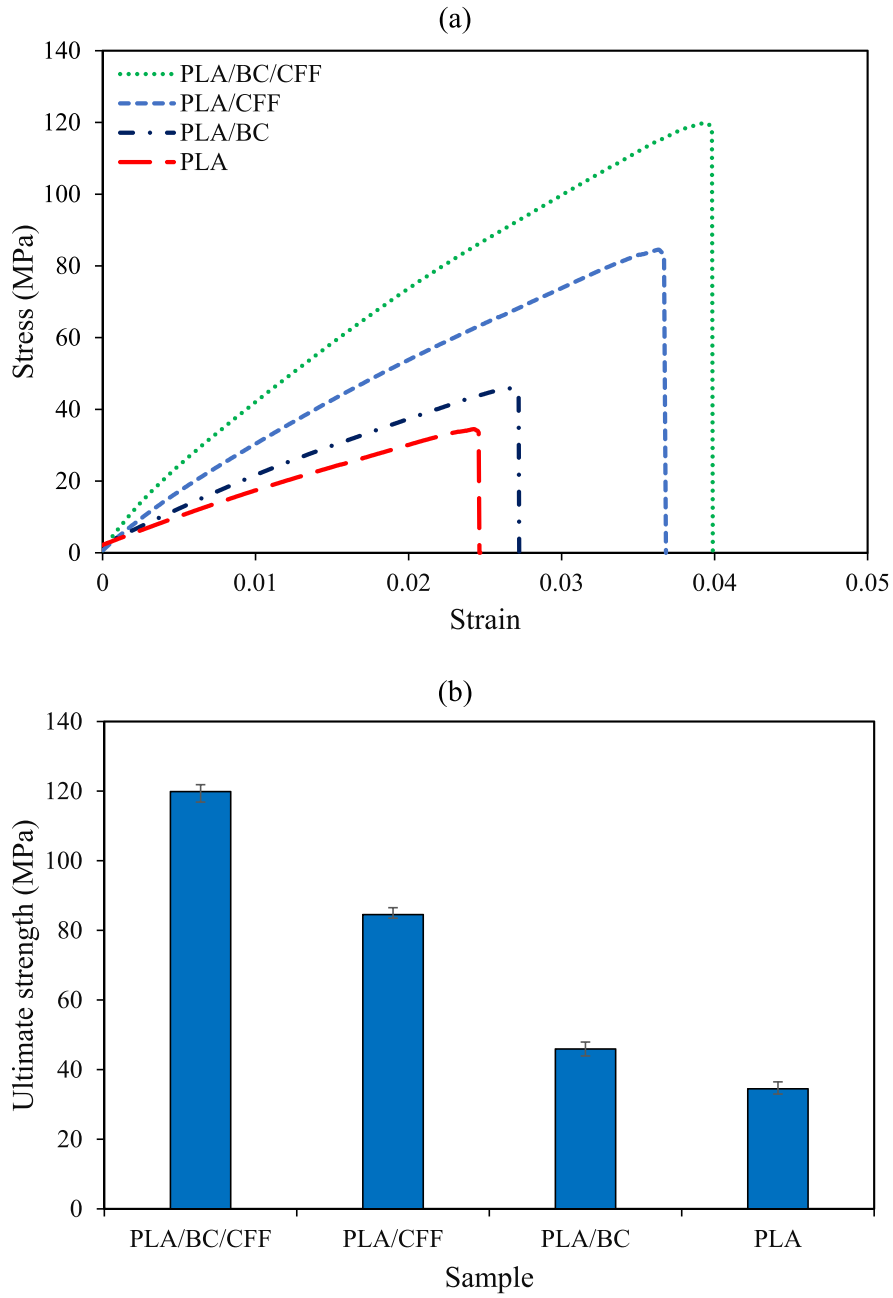

Fig. 8. (a) Tensile stress-strain behaviours of various printed materials (median values), (b) their average ultimate tensile strength.

specimens. As can be observed in the images, there is robust contact at the fibre-matrix interface, with minimal voids, indicating good impregnation and wet-out in the samples. During the tensile tests, sections of the matrix experienced fracture and damage due to the applied tensile stress. This fracture and damage include fibre breakage, with some fibrils being pulled out from the flax fibres. In another section, BC particles are observed at the interface, where they may enable crack-stopping (or diverting) mechanisms. This phenomenon may explain the increase in strength observed when BC is added to PLA and PLA/CFF.

The strong bonding observed at the fibre-matrix interface in Fig. 10a can be attributed to the chemical and mechanical interlocking between the PLA matrix and the flax fibres. The flax fibres enhance the interfacial adhesion by increasing the surface roughness and promoting compatibility with the PLA matrix, leading to an effective stress transfer during the mechanical loading. The crack formation and propagation, as seen in the SEM images, are primarily due to the brittle nature of the PLA matrix, which fractures under tensile stress. However, the presence of well-dispersed BC particles at the interface contributes to crack-stopping and crack-diverting mechanisms, effectively mitigating crack growth and enhancing the composite's resistance to failure. The fibre pull-out phenomenon is indicative of the matrix's partial failure to hold the fibres in place during fracture. This occurrence is typically associated with the relative weakness of the matrix compared to the fibre strength, but it also reflects the energy dissipation mechanism that contributes to the composite's toughness.

Accurately determining the fibre volume fraction is crucial for the development of printed composites and serves as a fundamental indicator of composite quality, impacting its mechanical properties and performance. Therefore, the volume fraction of flax fibres in the PLA bio-composite was determined using ImageJ software. To achieve this, a cross-section of an as-manufactured (PLA/BC/CFF bio-composite) sample was cut. The cross-section was divided into three parts, and SEM

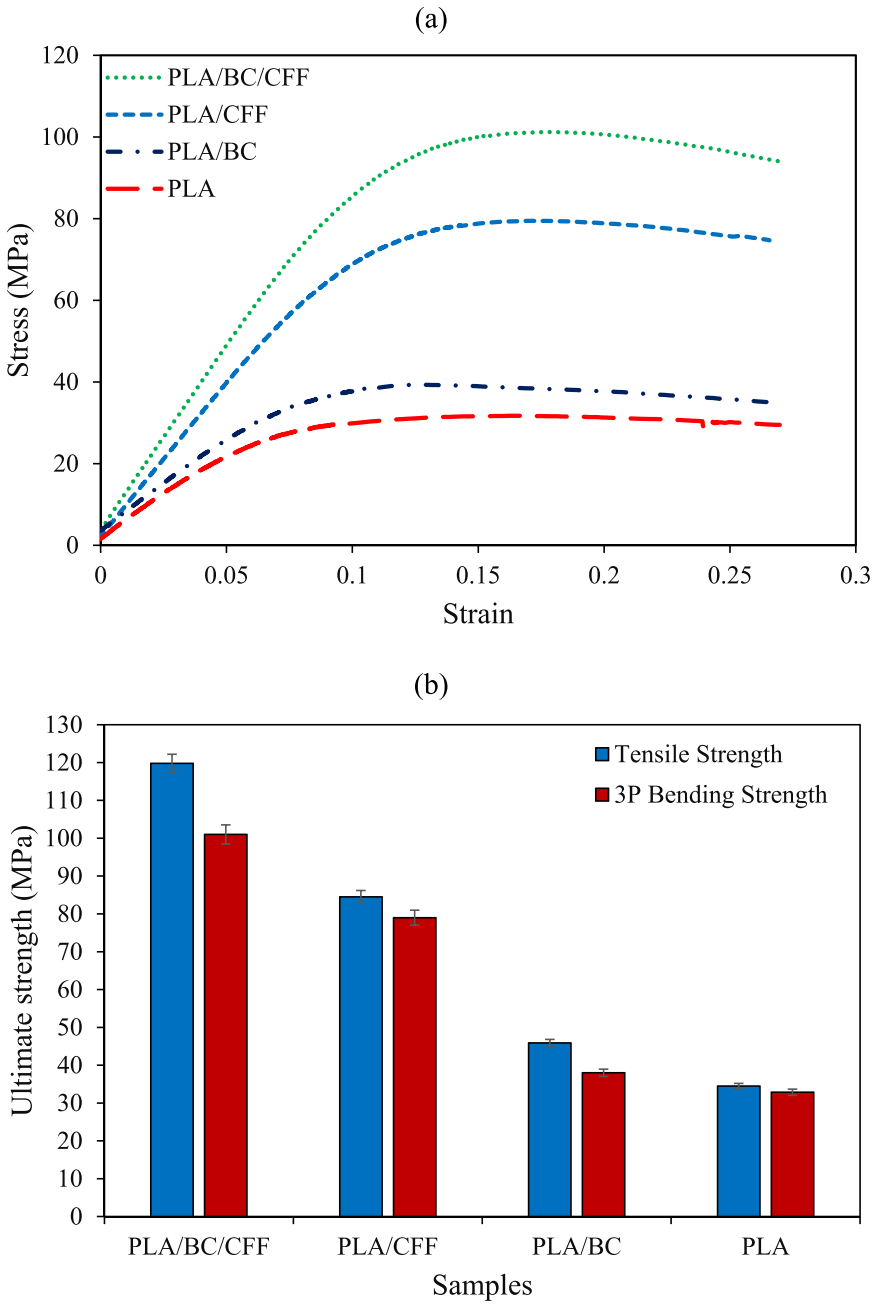

Fig. 9. (a) Three-point bending behaviours of various printed materials (b) ultimate (i.e., maximum), strength values from three-point bending tests versus tensile tests.

images of each section were taken. The images were analysed using ImageJ software, as shown in Fig. 10b, to estimate and assess the percentage of flax fibres (i.e., the fibre volume fraction). The average value of the flax fibre volume fraction was approximately 48 %. The same process was performed for the PLA/CFF composite sample producing outcomes that are comparable to the PLA/BC/CFF sample.

5.4. Dynamic mechanical analysis

The storage modulus and T_g are two important thermodynamic parameters related to the SME in SMPBs. These parameters need to be measured to evaluate the shape memory behaviour resulting from the mechanical properties of 4D-printed samples. It is also essential to investigate the effect of adding CFF and BC particles on the storage modulus and T_g of PLA. To perform these investigations, a DMA was used to analyse pure PLA and 3D/4D-printed SMPBs. The storage modulus and tan δ values for pure PLA and SMPBs are illustrated In Fig. 11a and b, respectively. The prominent peak in tan δ is associated with the glass transition temperature. In comparison to pure PLA, the results show a considerable increase in storage modulus in SMPBs. Furthermore, the reinforced PLA has a lower peak value of tan δ than pure PLA, showing that the printed composites are stronger and stiffer than pure PLA. Also, as seen in Fig. 11b, the T_g for pure PLA is about 63 °C, while for PLA/BC/CFF, PLA/CFF, and PLA/BC, it reads approximately 64.3, 65.3, and 65.8 °C, respectively. To ensure consistent performance in shape memory characteristics, all samples were tested at temperatures above their T_g.

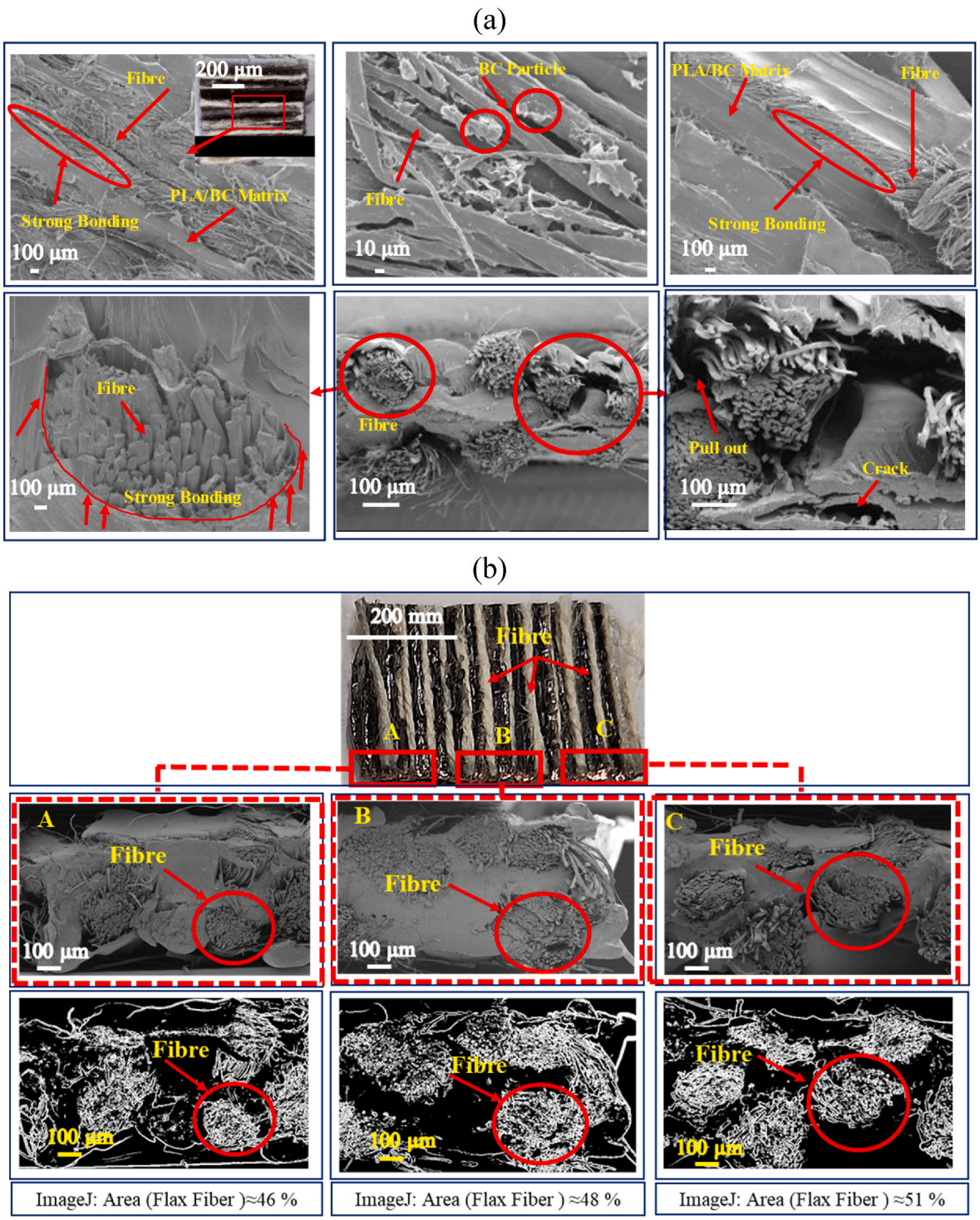

Fig. 10. (a) SEM microphotograph of the PLA/BC/CFF bio-composite, (b) determination of fibre volume fraction of the PLA/BC/CFF composite by using ImageJ software.

5.5. MFI of PLA/BC composite

The MFI of the PLA reads 12 g/10 min. The melt flow of the PLA composite reduces to 9 g/10 min after adding 3 wt% BC particles. It means this composite reinforcement decreases the MFI by 33 %. The lower MFI can be attributed to the interaction of the PLA and BC particles that restricts the movement of the polymer chains. It results in a drop in the flowability of the PLA/BC composite. However, the PLA/BC composite still has a good level of printability and can also be integrated with the continuous fibre.

5.6. Flammability properties

In this section, the flammability properties of the printed bio-composites are investigated by UL-94 horizontal and vertical burning tests, LOI and CC tests as presented in Fig. 12 and Table 3. Firstly, the bio-composite samples are examined under UL-94 horizontal burning test. Fig. 12a and b shows the appearance of sample after burning and

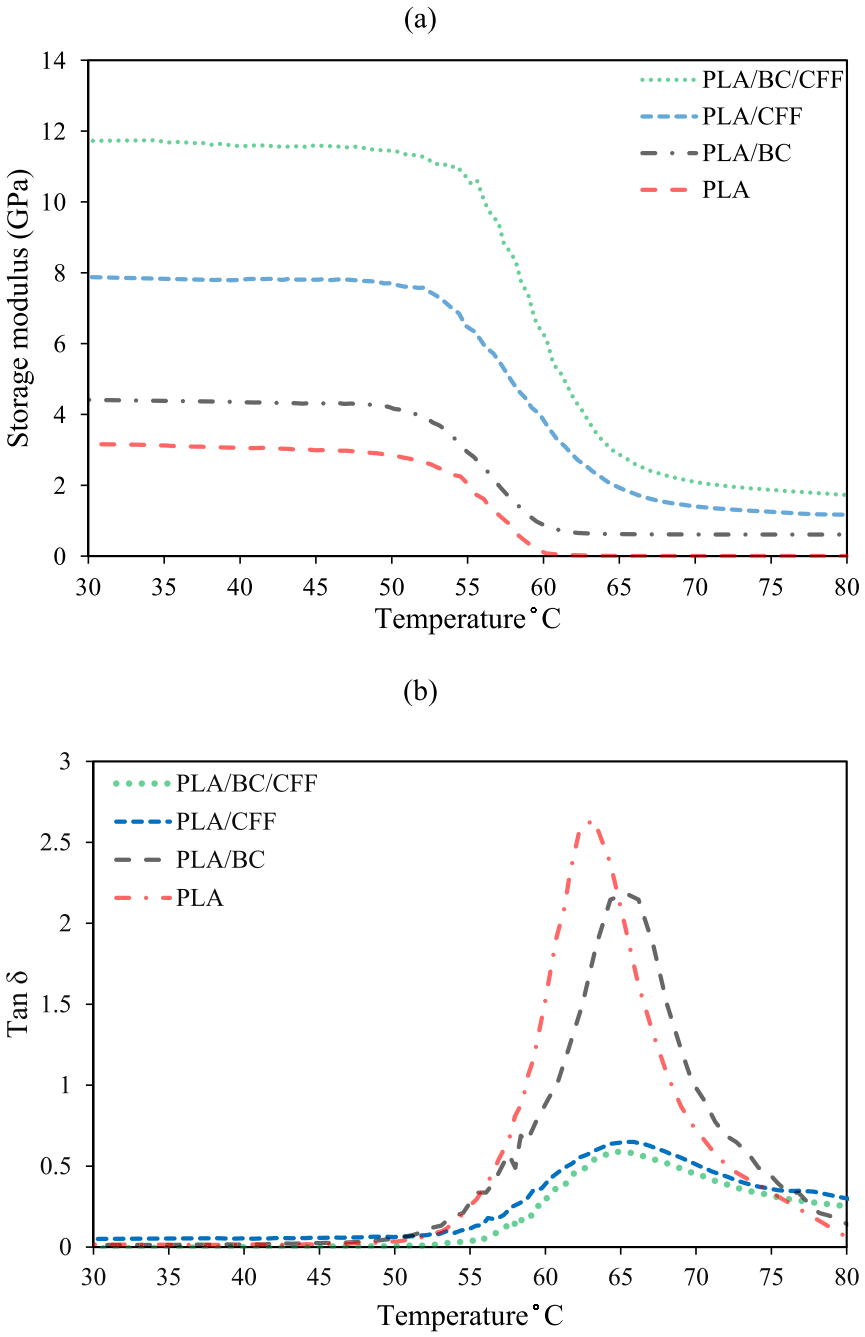

Fig. 11. DMA finding in terms of (a) storage modulus and (b) tan δ for printed samples.

the average burning rates of the bio-composites. Fig. 12a illustrates how the samples looked post-burning. As can be seen, the samples reinforced with CFF did not burn completely, whereas the samples without flax fibres burned entirely. Fig. 12b also presents the average burning rates of the bio-composites. Among the developed samples, PLA/BC/CFF and PLA/CFF exhibit the lowest burning rates, with improvements of 50 % and 45 %, respectively, compared to the pure PLA. The reduction in burning rate can be attributed to the presence of natural fibres and BC particles, which form protective layers that prevent the penetration of heat and volatile substances into the inner layers of the composite. The improved flame retardancy properties observed with the addition of BC and CFF result from their synergistic effects on reducing flammability. BC acts as a thermal barrier by forming a protective char layer during combustion, which slows the transfer of heat and oxygen to the underlying layers and traps volatile gases, preventing their escape and subsequent fuelling of the flame. Meanwhile, CFF contribute to the structural integrity of the composite and enhance the formation of the protective layer by providing reinforcement. Together, BC and CFF restrict the penetration of heat and flames, leading to lower burning rates and incomplete combustion of the reinforced composites compared to the pure PLA. In contrast, the pure PLA sample shows the highest burning rate. This higher rate could be due to the rapid thermal degradation of PLA during burning, making it more susceptible to flames. The PLA/BC sample proves a lower burning rate than pure PLA, with 30 % improvement. Based on the data obtained in this section and the mechanical properties section, it is clear that adding BC particles and continuous CFF fibres to PLA enhances both mechanical strength and flame retardance.

Secondly, the flame retardancy of PLA and bio-composites is evaluated via UL-94 and LOI tests, and the results are presented in Table 3.

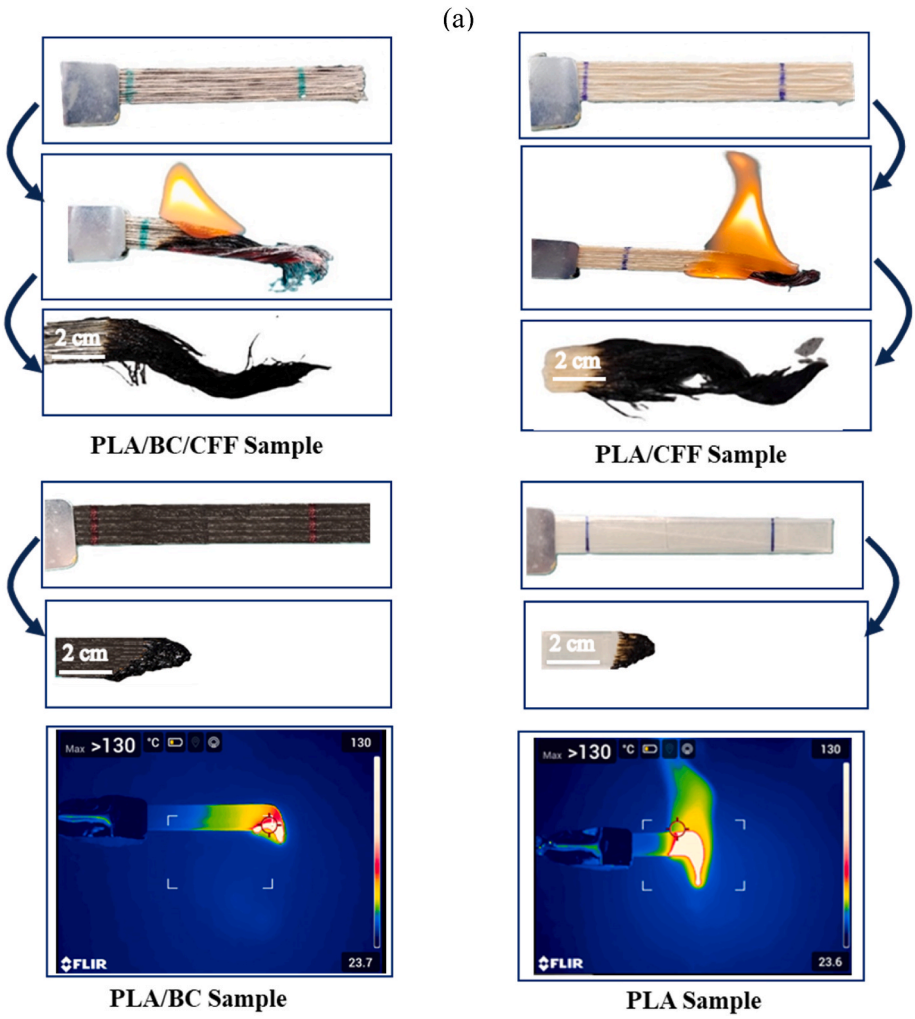

Fig. 12. (a) Visual documentation of clamping specimen and igniting it, (b) the burning rate assessment of printed composites, (c, d) typical CCT curves including the HRR and THR of PLA, PLA/BC, PLA/CFF, and PLA/BC/CFF bio-composites.

The UL-94 results show that the fire performance of PLA/CFF and PLA/BC/CFF is improved significantly from no rating to V-2 and V-1 rating, respectively. This reveals that the effect of CFF is more pronounced when added to PLA, and PLA/CFF and PLA/BC/CFF have medium and high improved rating. Also, it is seen from Table 3 that the LOI of bio-composites increases via the reinforcement of BC and CFF. For example, adding CFF and BC/CFF to PLA increases the LOI respectively to 33.6 % and 36.8%vol. compared to the pure PLA (20.5%vol). This increase can be associated with the reinforcements to form char which acts as a barrier to the heat transfer.

To better understand the improved flame retardancy properties of bio-composites under specific combustion conditions, CCTs were carried out. The key parameters measured in CCTs include time to ignition (TTI), peak heat release rate (pHRR), and total heat release (THR), as presented in Table 3 and illustrated in Fig. 12c and d. As shown in Table 3, the addition of BC and CFF delays TTI. The pure PLA has a TTI of 56 s, which increases to 73 s for the PLA/BC/CFF composite. This delay can be attributed to the uniform distribution of BC and the effective PLA coating of CFF, which facilitate the formation of a protective char layer acting as a barrier to the heat transfer. The effectiveness of all flame retardants can also be clearly seen from HRR and THR versus time curves in Fig. 12c and d. Fig. 12 c displays double-peaked heat release rate curves for the bio-composites reinforced with CFF, a typical behaviour observed in cellulosic fibre-reinforced composites. The first peak corresponds to the initial burning of sample after ignition. During this phase, the CFF and BC begin to char, forming a charred layer that serves as a thermal barrier, slowing down the combustion of the underlying polymer. The pHRR values for PLA/CFF and PLA/BC/CFF are 280 kW/m^2 and 234 kW/m^2, respectively, representing reductions of 51 % and 80 % compared to the pure PLA. Moreover, the THR value for PLA/BC/CFF decreases significantly from 104.2 MJ/m^2 to 50 MJ/m^2 compared to the pure PLA, as shown in Table 3 and Fig. 12d.

These results highlight the potential use of 3D-printed flame-retardant bio-composites reinforced with plant-based resources and CFF as sustainable and eco-friendly materials for various industries such as automotive, logistics, construction, and furniture. Specifically, in flame-retardant designs like transportation units, cabins, or house interior furniture, these bio-composites could contribute to more sustainable and safer product design and environment.

5.7. Shape memory features

This section is dedicated to study the SME of various bio-composites and investigate the influence of the CP and HP protocols and natural reinforcements including BC particles and CFF on shape fixation and recovery performance. The samples were placed vertically, and their shape memory behaviour was evaluated. Temperature was measured using an infrared camera. As a visual example, Fig. 13a, b illustrate the

(b)

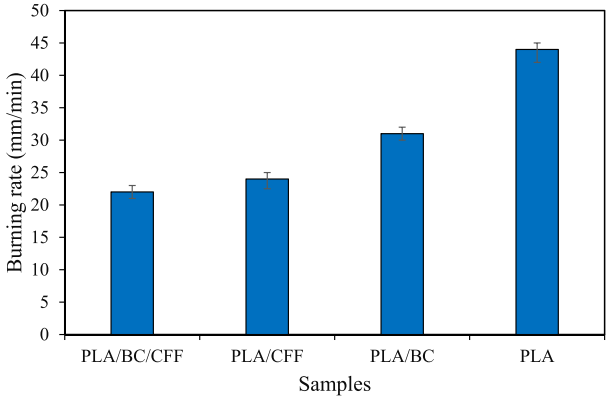

(c)

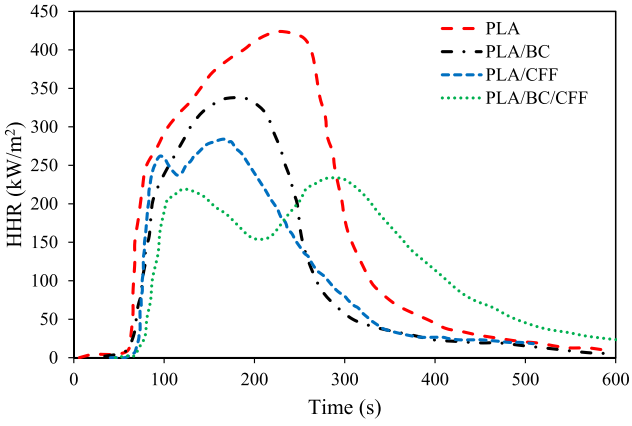

(d)

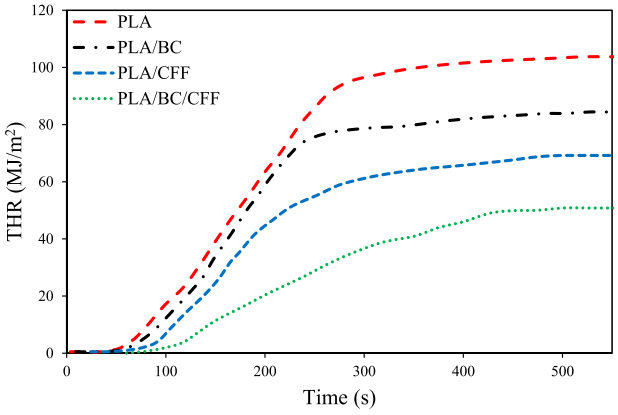

Fig. 12. (*continued*).

configuration of the PLA/CFF and PLA/BC/CFF printed samples at the end of HP protocol and during heat-induced recovery. The counterpart of this figure for the PLA/CFF and PLA/BC/CFF samples under CP protocol is presented in Fig. 13c and d. Comparing the configuration of samples at the end of CP/HP methods show that both composites are able to be programmed for a temporary shape. In this respect, shape fixation is much greater under the HP protocol. By heating via a heat gun, the samples return to their original shape revealing the SME. These figures also reveal that the inelastic deformation produced by loading and remained in the bio-composite after unloading is recoverable partially which is a great achievement for this class of materials.

Next the share memory behaviours of all the materials are investigated. Fig. 14a and b presents the average values for shape-fixity and shape-recovery ratios of the bio-composites. Fig. 14a illustrates the performance of SMPBs in maintaining the shape of samples trained under CP/HP methods. As can be seen, the HP approach improves the ability of the materials to retain their shape and results in a higher shape fixation performance compared with the CP protocol for all material types. Pure PLA shows the highest shape fixation ability under both HP and CP protocols, while PLA/BC/CFF has the lowest values for HP and CP. It can be concluded that reinforcing materials by long continuous fibres enhances the overall stiffness and resilience and reduces the shape

Table 3
UL-94 rating, LOI and CCT data for PLA and bio-composite.

Samples	UL-94		LOI (vol %)	TTI (s)	pHHR (kW/m^2)	THR (MJ/m^2)
	Dripping	Rating				
PLA	Yes	No rating	20.5	56	424	104
PLA/BC	Yes	No rating	25.3	61	337	83
PLA/CFF	Yes	V2	33.6	65	280	69
PLA/BC/CFF	Yes	V1	36.8	73	234	50

fixity capability. In fact, continuous fibres act like a spring and, once the load is removed from the material at the end of programming, they try to return to the initial shape and reduce the shape fixity index. Fig. 14b shows the shape recovery ratio for these composites once they are re-heated above their T_g to 77 °C and then cooled to the room temperature, 23 °C. Pure PLA has the best performance with shape recovery ratios of 96.9 % and 98.9 % in the CP and HP methods. PLA/BC also reveals a good performance with a shape recovery ratio close to pure PLA. In contrast, the printed PLA/BC/CFF composites result in the lowest shape recovery performance of 89 % and 82 % under HP and CP. Adding BC particles and CFF to PLA reduce the material's ability to recover its shape, causing a notable decline. A similar observation was reported by Zhang et al. [25] for BC-m/PLA composites. When results of micro and macro reinforcements by BC and CFF are compared, it can be concluded that reinforcement in the macro scale has a bigger negative impact on the shape recovery performance. Finally, Fig. 14c displays the speed of shape recovery for various bio-composites. It is found that PLA/BC/CFF possesses the fastest actuation performance among others with 4.5 s of shape recovery time. PLA/CFF comes to the second with 5 s shape recovery time, while PLA/BC and PLA require 6.5 and 7 s to recover their shapes. This comparison shows that reinforcing PLA can speed up the recovery time or actuation frequency. In this respect, the larger stiffness contribution from CFF results in a superior shape

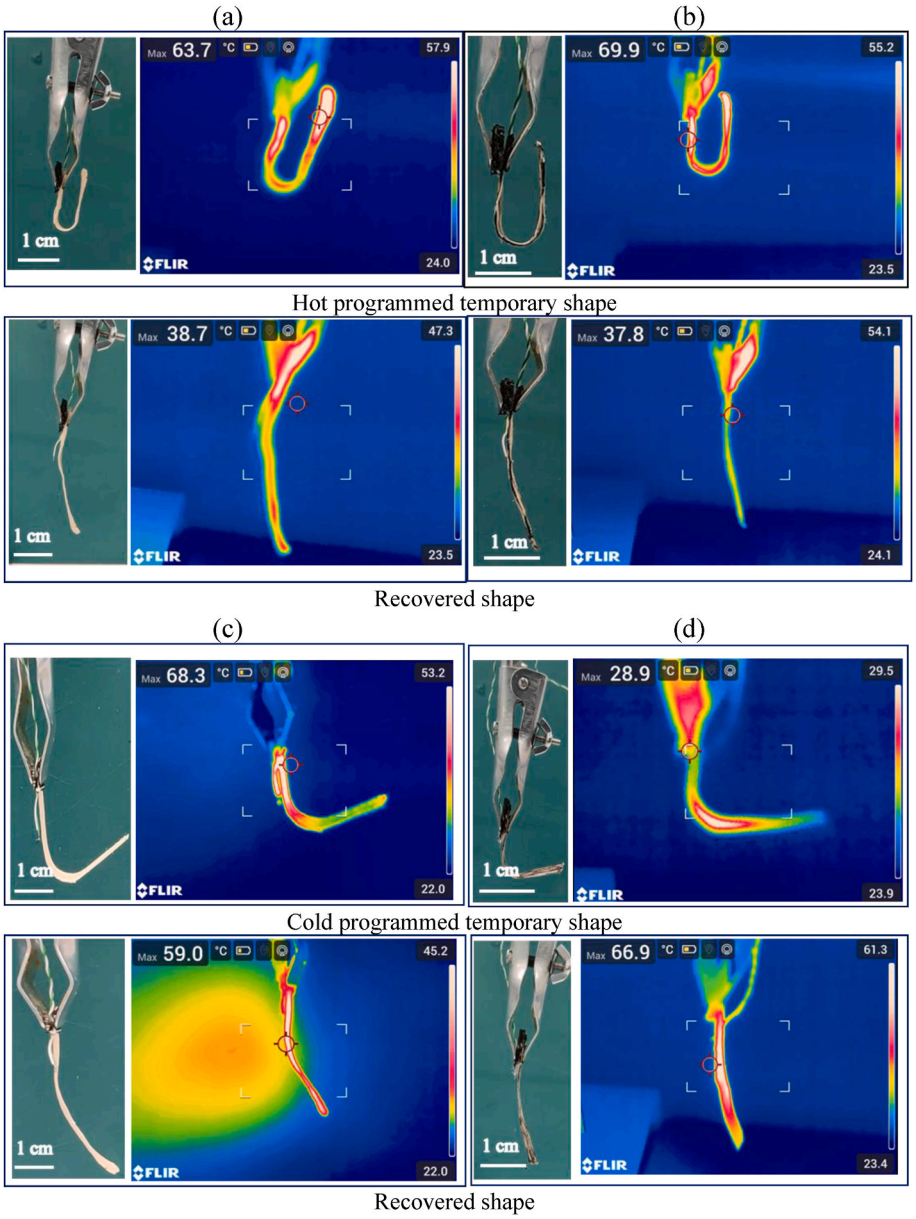

Fig. 13. Temporary shape (a) and heat-induced recovered shape (b) of the printed PLA/CFF and PLA/BC/CFF programmed under HP protocol, respectively. Temporary shape (c) and heat-induced recovered shape (d) of the printed PLA/CFF and PLA/BC/CFF programmed under CP protocol, respectively.

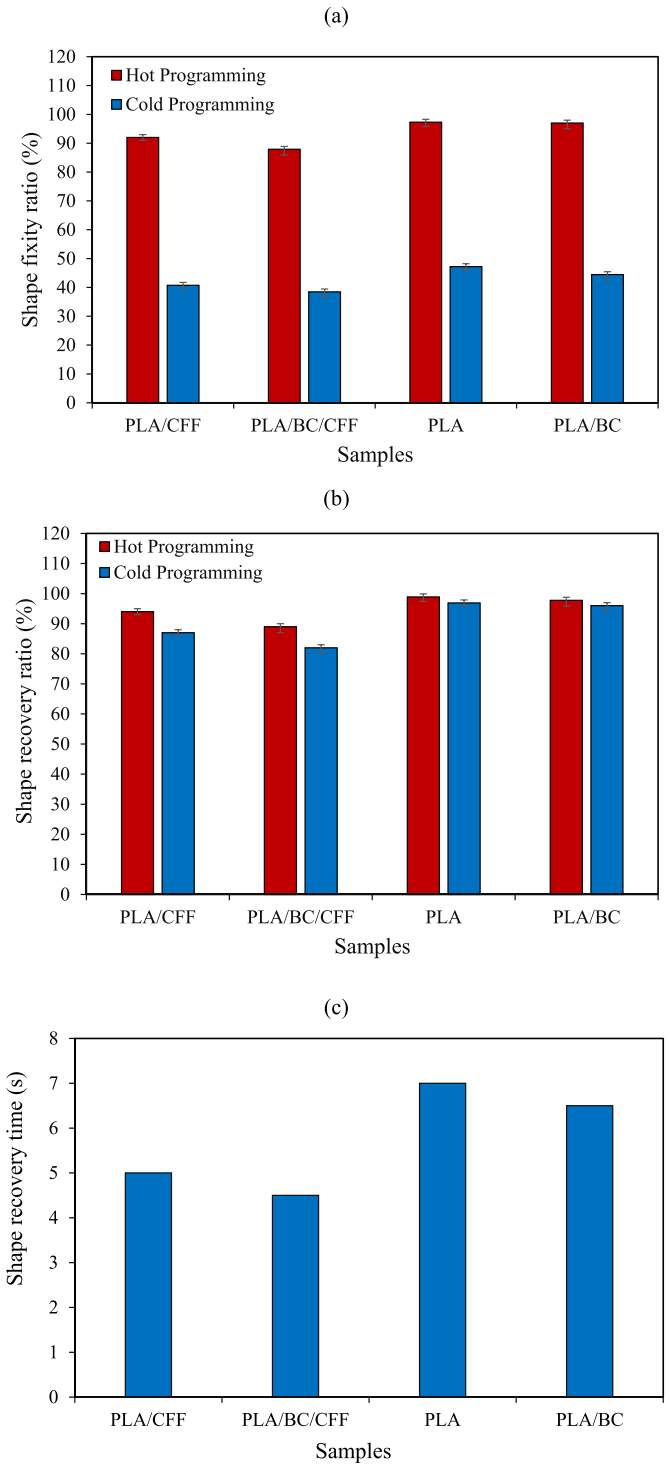

Fig. 14. Shape memory performance of bio-composites trained under CP/HP protocols in terms of (a) shape fixity ratio, (b) shape recovery ratio, (c) shape recovery time for HP.

recovery time when compared to BC particles.

6. Potential structural applications

6.1. Cellular meta-bio-composite structures

In recent years, 4D printing has gained attention in the field of additive manufacturing, focusing on sustainable product design and reducing materials consumption. FFF technology enables the fabrication of customised cost-effective products with potential reusability. Lattice or cellular meta-structures with hierarchical arrangements have also been developed for application across various industrial sectors due to their high specific strength and stiffness [39]. To show the capabilities of the PLA/BC/CFF bio-composite developed in this work for structural applications, a simple conceptual meta-structure design so-called meta-bio-composite was printed and investigated featuring lightweight, resilience, energy absorption/dissipation, and recoverability/reusability characteristics. The 2D meta-bio-composite with a circular cross-section was designed and printed as shown in Fig. 15a. The sample was trained via the CP protocol. It was first subjected to compressive loading and then unloading using the mechanical tester machine at a speed of 5 mm/min. Experiments was performed in triplicate and average values were reported for each series of tests in this section. The results in terms of force-displacement during loading and unloading are presented in Fig. 15b for various maximum compression levels of 75 %, 50 %, and 25 % (of the original height, 40 mm). Their shape recovery was also investigated by heating the loaded-unloaded samples above the T_g to 77 °C and then cooling to the room temperature, 23 °C.

The experimental observation showed that the meta-bio-composite under compression up to 75 % compression collapsed with major cracks. In contrast, the structure compressed to 50 % compression looked undamaged and was investigated further for a potential shape recovery as shown in Fig. 16. The structure was first loaded to achieve 50 % compression and then unloaded fully, showing a residual inelastic strain/deformation. The structure was then heated above the glass transition temperature to 77 °C and finally cooled down to the room temperature. Infrared images of the shape recovery process are presented in Fig. 16b. Fig. 16 shows that the residual inelastic strain is partially recoverable, and an 85 % shape recovery ratio can be achieved after the heating-cooling process. The reversibility and recovery of the mechanical properties were further investigated by applying another loading-unloading cycle to the recovered meta-bio-composite. Fig. 16c illustrates the force-displacement results of the first and second cycles for the sample subjected to maximum 50 % compression.

The force-displacement response of the meta-structure as presented in Figs. 15 and 16c are now discussed further in detail. It is seen that the meta-bio-composite experienced an almost linear elastic response in the beginning of the loading step until 10 mm displacement. The meta-structure then buckled and lost stability resulting in a force-displacement plateau. This general softening behaviour due to the overall collapse of the structure leads to a quasi-constant force response in which the structure stiffness approximately tends to zero (quasi-zero stiffness) and experiences further deformation under negligible applied load. Such behaviour is beneficial for two main applications. Firstly, the quasi-constant force meta-structure offers an over-load protection feature in which the impacting object does not experience higher forces, and the meta-structure could prevent any damage to the external impactor. In fact, the meta-structure acts like a regulator and offers a stable force output over a wide range of compression. This feature could also enhance comfort level in interaction between two objects. Secondly, the meta-structure with a quasi-zero stiffness feature could convert the input kinetic energy into the elastic and plastic energy, buckling-type mechanical instability and absorb/dissipate a significant amount of energy during compression without encountering excessive force/stress. As can be seen, further loading leads to a drop in the force value indicating further plastic flow deformation and a softening behaviour, see Fig. 15b at 15 mm compression. This plastic deformation also contributes to the energy dissipation. Further compression leads to a transition from softening to hardening due to densification and collision resistance phenomena.

Next, the structure is unloaded showing a mechanical hysteresis characterised by a noncoincident loading-unloading curve. The structure releases the absorbed energy and recovers the original shape fully or partially while some plastic deformations may remain in the material.

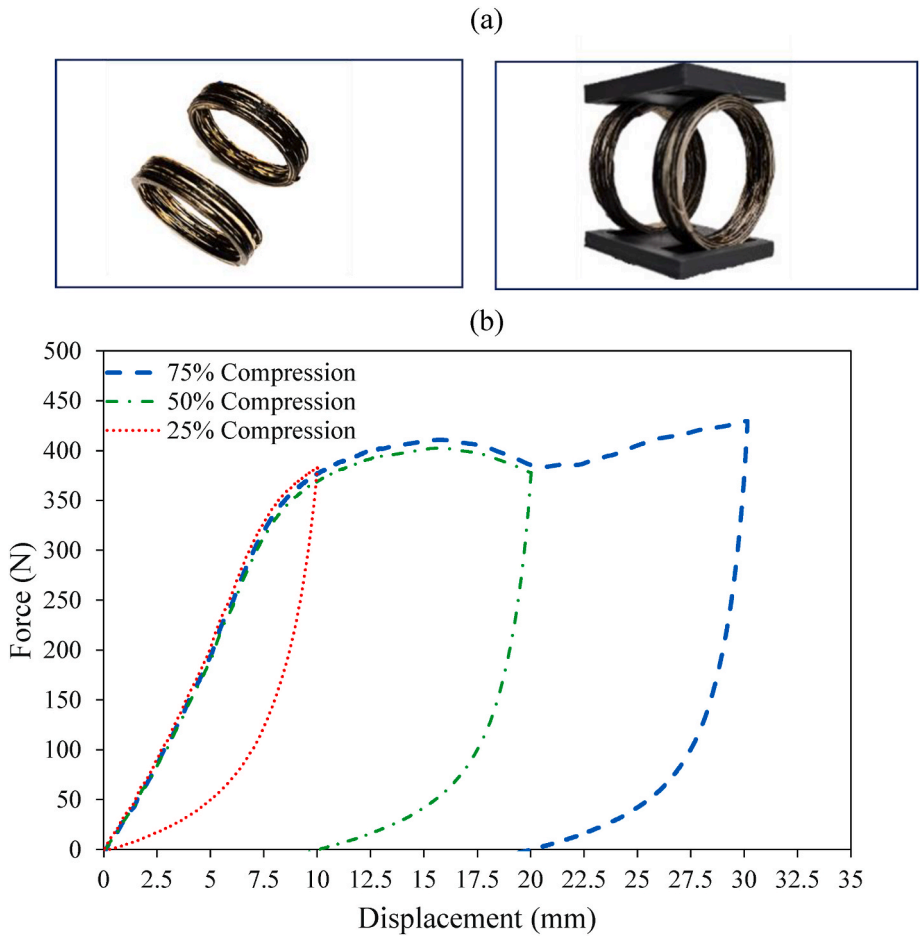

Fig. 15. (a) Cellular meta-bio-composite with a circular cross-section assembled sandwiched between two plates, (b) compression behaviours of the meta-structure under a loading-unloading cycle in terms of force-displacement for different maximum compression levels of 75 %, 50 %, and 25 %.

As can be seen, the meta-bio-composite loaded to 25 % compression could fully recover the original shape and dissipate some of the kinetic energy via hysteresis loop due to the buckling-type mechanical instability. While the plastic deformation in the sample loaded up to 75 % compression led to macroscopic cracks, the one loaded to a maximum of 50 % compression looked undamaged and could experience shape recovery through modest heating (to 80 °C). Its plasticity is partially recoverable as can be seen in Fig. 16. Interestingly, it is seen that the meta-bio-composite could experience a second loading-unloading cycle without significant change in behaviour. The linear elastic behaviour is almost the same while there is a minor 12 % drop in the quasi-constant force level, the hysteresis width and area, and consequently in the energy absorption/dissipation capacity. It reveals an acceptable recovery of mechanical properties for this newly developed bio-composite.

The amount of energy absorbed and dissipated over two cycles in samples compressed up to 50 % is demonstrated Fig. 17a. The yellow and green areas under the loading and unloading curves show the energy dissipation and absorption, respectively. Additionally, the specific energy absorption (SEA) was evaluated for the meta-bio-composites and presented in Fig. 17b. More details on SEA calculation can be found in Dezaki et al. [40]. The results presented in Fig. 17 reveal that the meta-bio-composite is capable of dissipating the majority of the kinetic energy. The meta-bio-composite still shows a high level of energy dissipation in the second cycle with just a 12 % drop in force compared with the first cycle.

Meta-bio-composites developed through 3D/4D printing present a powerful combination of advanced features that make them ideal for high-performance applications. These materials provide energy absorption, dissipation, and reusability, ensuring impact resistance and overload protection due to their constant-force and quasi-zero stiffness behaviour. Their ability to regulate force during deformation not only prevents excessive stress but also offers comfort, making them suitable for ergonomic designs. The incorporation of continuous natural fibres, such as flax, enhances the mechanical strength and lightweight nature of the composites, while bamboo charcoal improves flame retardancy, allowing their use in safety-focused areas like transportation units, cabins, automotive interiors and furniture. Moreover, the shape memory properties of these meta-bio-composites enable reversibility and recovery of mechanical properties, allowing deformed structures to regain their shape and strength after loading. This ensures extended usability and reduces material waste, aligning with sustainable manufacturing practices. The combination of high strength, lightweight, energy efficiency, and environmental sustainability makes these composites highly versatile, promising significant potential for industries such as automotive, aerospace, logistics, construction, and furniture, where durability, safety, and comfort are essential.

7. Concluding remarks

This study investigated the development of environmentally friendly flame-retardant bio-composites using 3D/4D printing technology by combining PLA, bamboo charcoal, and continuous flax fibres. The bio-composites showed significant improvements in mechanical properties, flame retardancy, and shape memory behaviour, positioning them as strong candidates for sustainable, high-performance applications. The key findings and achievements are summarised as follows.

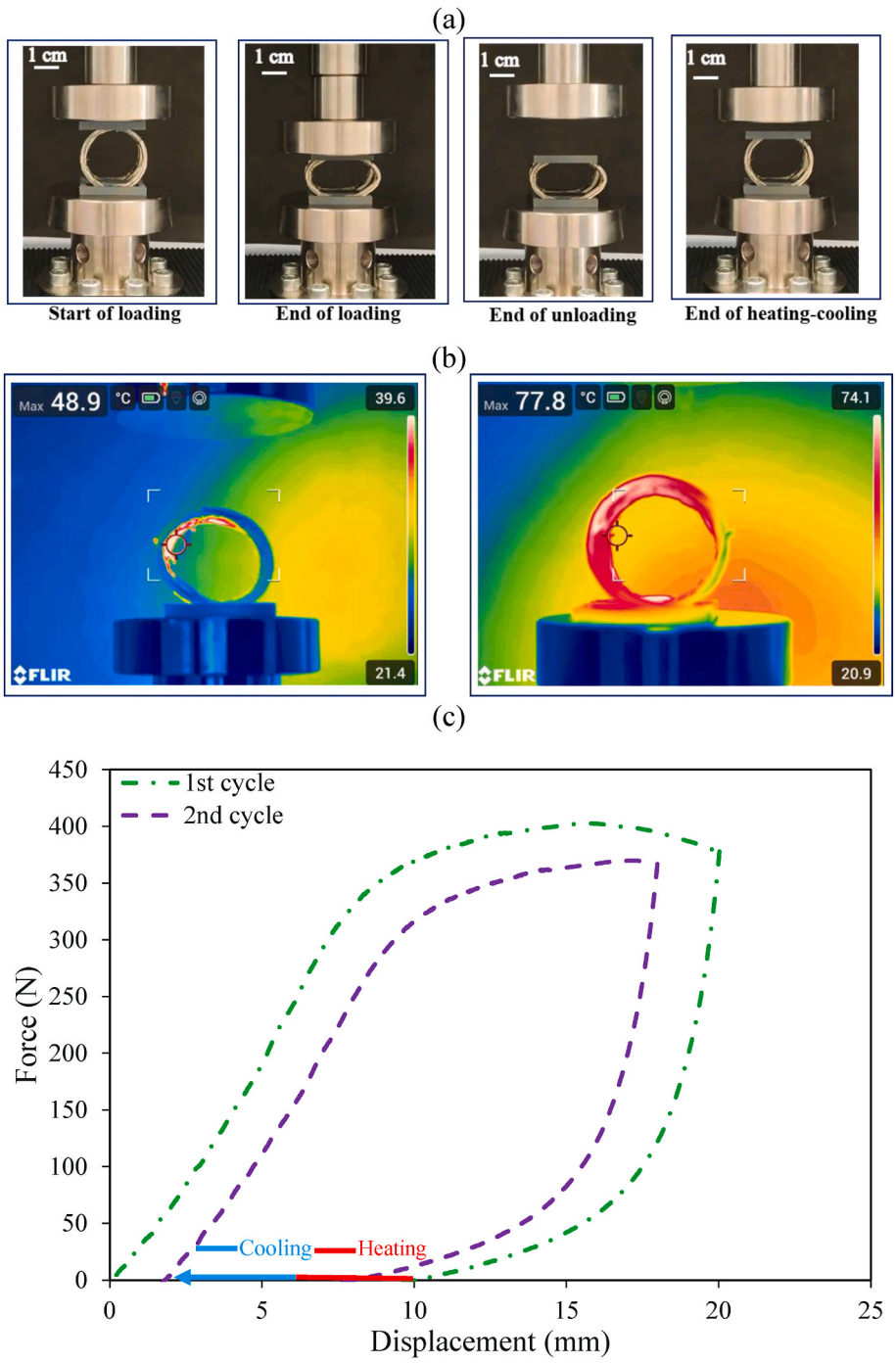

Fig. 16. (a) Configuration of the PLA/BC/CFF meta-bio-composite during loading up to 50 % compression, then unloading, and finally at the end of heating-cooling process, (b) infrared images captured during the shape recovery process achieving a shape recovery ratio of 85 %, (c) force-displacement response of the meta-bio-composite during the first loading-unloading cycle, heating-cooling (represented by the red-blue solid line), and then the second loading-unloading cycle.

- Mechanical Properties:
  - o The tensile strength of the PLA/BC/CFF composite increased by 248 %, while flexural strength improved by 207 % compared to pure PLA.
  - o Reinforcement with CFF enhanced the mechanical performance due to effective load transfer at the fibre-matrix interface, as observed in the microstructure through SEM analysis.
- Flame Retardancy Properties:
  - o The flame-retardant properties were notably improved, with a 50 % reduction in the burning rate after adding 3 wt% BC and CFF to PLA.
  - o The composites demonstrated enhanced flame resistance without compromising mechanical integrity, making them suitable for safety-critical applications.
  - o The LOI value and rating of UL-94 respectively reached 36.8%vol. and V-1 rating for PLA/BC/CFF bio-composite.
- Shape Memory Properties:
  - o Shape memory tests under CP and HP programming protocols showed efficient shape fixation and recovery.
  - o The shape recovery ratios reached 98.9 % and 96.9 % for pure PLA and 89 % and 82 % for PLA/BC/CFF composites under HP and CP,

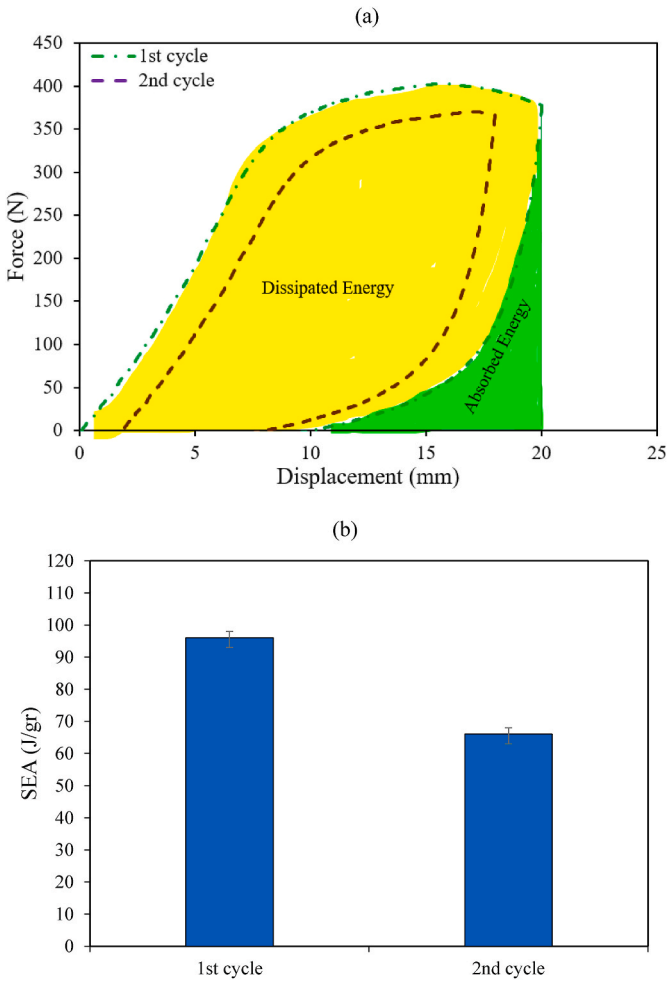

Fig. 17. (a) Force-displacement response during the first and second loading-unloading cycles showing dissipated and absorbed energies, (b) SEA calculated for two loading-unloading cycles.

respectively, highlighting their suitability for actuation and reconfigurability in 4D printing applications.
  - o The shape recovery time was reduced to 4.5 s for PLA/BC/CFF composites, further emphasising their enhanced performance in dynamic conditions.
- Energy Absorption/Dissipation:
  - o The meta-bio-composite compressed under 25 % compression dissipated energy leveraging a mechanical hysteresis, and fully recovered all deformations.
  - o The meta-bio-composite design exhibited quasi-zero stiffness and constant force behaviours, which are beneficial for applications requiring overload protection, force regulation and comfort.
  - o The meta-bio-composite under 50 % compression revealed 85 % shape recovery and demonstrated excellent energy absorption and dissipation, with only a 12 % drop in energy dissipation between the first and second loading cycles, ensuring consistent performance under cyclic loads.
- Sustainability and Lightweight:
  - o The bio-composite's lightweight nature, attributed to the use of natural fibres, coupled with their enhanced mechanical and thermal properties, contributes to sustainable manufacturing practices.
  - o These materials offer a promising alternative to synthetic composites, aligning with the principles of the circular economy and environmental responsibility.

In conclusion, the developed PLA/BC/CFF bio-composites provide a versatile solution for industries such as automotive, aerospace, logistics, construction, and furniture. Their high mechanical strength, flame retardancy, and shape memory properties, combined with energy absorption/dissipation characteristics, make them suitable for applications demanding durability, force/stress regulation, comfort/safety, and sustainability.

CRediT authorship contribution statement

Mahdi Bodaghi: Writing – review & editing, Writing – original draft, Supervision, Project administration, Methodology, Investigation, Funding acquisition, Formal analysis, Data curation, Conceptualization. **Kaveh Rahmani:** Writing – review & editing, Writing – original draft, Visualization, Methodology, Investigation, Data curation, Formal analysis. **Mohammadreza Lalegani Dezaki:** Writing – review & editing, Methodology, Investigation, Data curation, Formal analysis, Visualization. **Callum Branfoot:** Writing – review & editing, Methodology, Investigation, Formal analysis, Data curation. **Jon Baxendale:** Writing – review & editing, Methodology, Investigation, Formal analysis.

Declaration of competing interest

The authors declare that they have no known competing financial interests or personal relationships that could have appeared to influence the work reported in this paper.

Acknowledgements

The authors acknowledge the support by the Engineering and Physical Sciences Research Council (EPSRC) [Award Number: EP/Y011457/1], the EPSRC's Innovation Launchpad Network + Researcher in Residence scheme [Project: RIR26C230615-6, Researcher: Mahdi Bodaghi], and the RAEng/Leverhulme Trust Research Fellowship [Award Number: LTRF-2324-20-129].

Data availability

Data will be made available on request.

References

[1] F. Van Der Klift, Y. Koga, A. Todoroki, M. Ueda, Y. Hirano, R. Matsuzaki, 3D printing of continuous carbon fibre reinforced thermo-plastic (CFRTP) tensile test specimens, Open J. Compos. Mater. 6 (1) (2015) 18–27.
[2] C. Tóth, Á.D. Virág, L.M. Vas, N.K. Kovács, Prediction and analysis of flexural stiffness for 3D-printed continuous fiber–reinforced composites with different matrix fill ratios and layer orders, Polym. Test. 135 (2024) 108459.
[3] M. Heidari-Rarani, M. Rafiee-Afarani, A. Zahedi, Mechanical characterization of FDM 3D printing of continuous carbon fiber reinforced PLA composites, Compos. B Eng. 175 (2019) 107147.
[4] H. Mei, Z. Ali, I. Ali, L. Cheng, Tailoring strength and modulus by 3D printing different continuous fibers and filled structures into composites, Adv. Compos. Hybrid Mater. 2 (2019) 312–319.
[5] K.L. Pickering, M.A. Efendy, T.M. Le, A review of recent developments in natural fibre composites and their mechanical performance, Compos. Appl. Sci. Manuf. 83 (2016) 98–112.
[6] M. Jawaid, H.A. Khalil, Cellulosic/synthetic fibre reinforced polymer hybrid composites: a review, Carbohydr. Polym. 86 (1) (2011) 1–18.
[7] W. Ahmed, F. Alnajjar, E. Zaneldin, A.H. Al-Marzouqi, M. Gochoo, S. Khalid, Implementing FDM 3D printing strategies using natural fibers to produce biomass composite, Materials 13 (18) (2020) 4065.
[8] H. Zhang, D. Liu, T. Huang, Q. Hu, H. Lammer, Three-dimensional printing of continuous flax fiber-reinforced thermoplastic composites by five-axis machine, Materials 13 (7) (2020) 1678.
[9] S.K.S. Turjo, M.F. Hossain, M.S. Rana, M.S. Ferdous, Mechanical characterization and corrosive impacts of natural fiber reinforced composites: an experimental and numerical approach, Polym. Test. 125 (2023) 108108.
[10] O. Faruk, A.K. Bledzki, H.-P. Fink, M. Sain, Biocomposites reinforced with natural fibers: 2000–2010, Prog. Polym. Sci. 37 (11) (2012) 1552–1596.
[11] J. Merotte, A. Le Duigou, A. Kervoelen, A. Bourmaud, K. Behlouli, O. Sire, C. Baley, Flax and hemp nonwoven composites: the contribution of interfacial bonding to improving tensile properties, Polym. Test. 66 (2018) 303–311.

[12] V. Prasad, A. Alliyankal Vijayakumar, T. Jose, S.C. George, A comprehensive review of sustainability in natural-fiber-reinforced polymers, Sustainability 16 (3) (2024) 1223.
[13] M.N. Ahmad, M.R. Ishak, M. Mohammad Taha, F. Mustapha, Z. Leman, A review of natural fiber-based filaments for 3D printing: filament fabrication and characterization, Materials 16 (11) (2023) 4052.
[14] J.A. Taborda-Ríos, O. López-Botello, P. Zambrano-Robledo, L.A. Reyes-Osorio, C. Garza, Mechanical characterisation of a bamboo fibre/polylactic acid composite produced by fused deposition modelling, J. Reinforc. Plast. Compos. 39 (23–24) (2020) 932–944.
[15] D. Depuydt, M. Balthazar, K. Hendrickx, W. Six, E. Ferraris, F. Desplentere, J. Ivens, A.W. Van Vuure, Production and characterization of bamboo and flax fiber reinforced polylactic acid filaments for fused deposition modeling (FDM), Polym. Compos. 40 (5) (2019) 1951–1963.
[16] M.-p. Ho, K.-t. Lau, H. Wang, D. Hui, Improvement on the properties of polylactic acid (PLA) using bamboo charcoal particles, Compos. B Eng. 81 (2015) 14–25.
[17] W. Ahmed, F. Alnajjar, E. Zaneldin, A. Al-Marzouqi, M. Gochoo, S. Khalid, Implementing FDM 3D printing strategies using natural fibers to produce biomass composite, Materials 13 (2020) 4065.
[18] T. Letcher, M. Waytashek, Material property testing of 3D-printed specimen in PLA on an entry-level 3D printer. ASME International Mechanical Engineering Congress and Exposition, American Society of Mechanical Engineers, 2014. V02AT02A014.
[19] A. Le Duigou, A. Barbé, E. Guillou, M. Castro, 3D printing of continuous flax fibre reinforced biocomposites for structural applications, Mater. Des. 180 (2019) 107884.
[20] D. Lau, Q. Qiu, A. Zhou, C.L. Chow, Long term performance and fire safety aspect of FRP composites used in building structures, Construct. Build. Mater. 126 (2016) 573–585.
[21] S. Matkó, A. Toldy, S. Keszei, P. Anna, G. Bertalan, G. Marosi, Flame retardancy of biodegradable polymers and biocomposites, Polym. Degrad. Stabil. 88 (1) (2005) 138–145.
[22] H.G. Kim, B.C. Bai, S.J. In, Y.-S. Lee, Effects of an inorganic ammonium salt treatment on the flame-retardant performance of lyocell fibers, Carbon letters 17 (1) (2016) 74–78.
[23] A. Sienkiewicz, P. Czub, Flame retardancy of biobased composites—research development, Materials 13 (22) (2020) 1–30.
[24] C.E. Hobbs, Recent advances in bio-based flame retardant additives for synthetic polymeric materials, Polymers 11 (2) (2019) 224.
[25] L. Zhang, W. Chai, W. Li, K. Semple, N. Yin, W. Zhang, C. Dai, Intumescent-grafted bamboo charcoal: a natural nontoxic fire-retardant filler for polylactic acid (PLA) composites, ACS Omega 6 (41) (2021) 26990–27006.
[26] W. Li, L. Zhang, W. Chai, N. Yin, K. Semple, L. Li, W. Zhang, C. Dai, Enhancement of flame retardancy and mechanical properties of polylactic acid with a biodegradable fire-retardant filler system based on bamboo charcoal, Polymers 13 (13) (2021) 2167.
[27] N.P.G. Suardana, M.S. Ku, J.K. Lim, Effects of diammonium phosphate on the flammability and mechanical properties of bio-composites, Mater. Des. 32 (4) (2011) 1990–1999.
[28] B.K. Kandola, W. Pornwannachai, J.R. Ebdon, Flax/pp and flax/pla thermoplastic composites: influence of fire retardants on the individual components, Polymers 12 (11) (2020) 2452.
[29] I. Vroman, L. Tighzert, Biodegradable polymers, Materials 2 (2009) 307–344.
[30] K. Sugimoto, T. Shinagawa, K. Kuroki, S. Toma, R. Hosomi, M. Yoshida, K. Fukunaga, Dietary bamboo charcoal decreased visceral adipose tissue weight by enhancing fecal lipid excretions in mice with high-fat diet-induced obesity, Preventive Nutrition and Food Science 28 (3) (2023) 246.
[31] ASTM D638-14-Standard Test Method for Tensile Properties of Plastics, ASTM, 2014.
[32] ASTM D3039-Standard Test Method for Tensile Properties of Polymer Matrix Composite Materials, ASTM International, 2017, p. 360.
[33] ASTM D790-Standard test methods for flexural properties of unreinforced and reinforced plastics and electrical insulating materials, Annu. Book ASTM Stand. (1997).
[34] ASTM D635-Standard Test Method for Rate of Burning And/or Extent and Time of Burning of Plastics in a Horizontal Position, ASTM International, West Conshohocken, PA, USA, 2003.
[35] M. Lalegani Dezaki, C. Branfoot, J. Baxendale, M. Bodaghi, Bio-based gradient composites for 3D/4D printing with enhanced mechanical, shape memory, and flame-retardant properties, Macromol. Mater. Eng. (2024) 2400276.
[36] M. Azlin, S. Sapuan, M. Zuhri, E. Zainudin, R. Ilyas, Thermal stability, dynamic mechanical analysis and flammability properties of woven kenaf/polyester-reinforced polylactic acid hybrid laminated composites, Polymers 14 (13) (2022) 2690.
[37] L. Lin, Q.A. Dang, H.E. Park, Enhanced degradability, mechanical properties, and flame retardation of poly (lactic acid) composite with New Zealand jade (pounamu) particles, Polymers 15 (15) (2023) 3270.
[38] S.-Y. Fu, X.-Q. Feng, B. Lauke, Y.-W. Mai, Effects of particle size, particle/matrix interface adhesion and particle loading on mechanical properties of particulate–polymer composites, Compos. B Eng. 39 (6) (2008) 933–961.
[39] M. Bodaghi, L. Wang, F. Zhang, Y. Liu, J. Leng, R. Xing, M.D. Dickey, S. Vanaei, M. Elahinia, S. Van Hoa, 4D printing roadmap, Smart Mater. Struct. 33 (11) (2024) 113501.
[40] M.L. Dezaki, M. Bodaghi, 4D printing and programming of continuous fibre-reinforced shape memory polymer composites, Eur. Polym. J. 210 (2024) 112988.